NAVAL POSTGRADUATE SCHOOL

MONTEREY, CALIFORNIA

THESIS

USING ACOUSTIC BACKSCATTER TO MEASURE SEDIMENT FLUX IN THE SURF ZONE

by

Preston J. Roland

December 2006

Thesis Advisor:	Timothy P. Stanton
Second Reader:	Edward B. Thornton

Approved for public release; distribution is unlimited.

THIS PAGE INTENTIONALLY LEFT BLANK

REPORT DOCUMENTATION PAGE		Form Approved OMB No. 0704-0188

1. AGENCY USE ONLY *(Leave blank)*	2. REPORT DATE December 2006	3. REPORT TYPE AND DATES COVERED Master's Thesis

4. TITLE AND SUBTITLE Using Acoustic Backscatter to Measure Sediment Flux in the Surf Zone	5. FUNDING NUMBERS
6. AUTHOR(S) Preston J. Roland	
7. PERFORMING ORGANIZATION NAME(S) AND ADDRESS(ES) Naval Postgraduate School Monterey, CA 93943-5000	8. PERFORMING ORGANIZATION REPORT NUMBER
9. SPONSORING /MONITORING AGENCY NAME(S) AND ADDRESS(ES) N/A	10. SPONSORING/MONITORING AGENCY REPORT NUMBER

11. SUPPLEMENTARY NOTES The views expressed in this thesis are those of the author and do not reflect the official policy or position of the Department of Defense or the U.S. Government.

12a. DISTRIBUTION / AVAILABILITY STATEMENT Approved for public release; distribution is unlimited.	12b. DISTRIBUTION CODE A

13. ABSTRACT (maximum 200 words)

Transport of sediment in coastal regions directly impacts mine countermeasure operations and naval construction efforts. Wave induced shear stress in the surf zone is responsible for entraining sediment particles into suspension within the combined wave and current boundary layer, where momentum is imparted through highly nonlinear processes. Therefore, a detailed understanding of sediment flux processes in the surf zone is essential to accurately model net sediment transport. This study examines the use of acoustic backscatter inversion as a means of measuring sediment concentration profiles. Measurements of sediment concentration and velocity profiles were made by a high frequency Doppler velocity profiler deployed on Black's Beach during the Nearshore Canyon Experiment, NCEX. Profiles of sediment flux were compared with hourly mean current measurements from a cross-shore/long-shore array of PUV sensors and two-dimensional planner images of the morphological evolution provided by a three camera Argus video suite.

Observations from a seven day period containing the development and evolution of a weak rip channel demonstrated that acoustic backscatter inversion techniques, when calibrated with *in situ* sediment samples, provide high spatial and temporal resolution estimates of sediment concentration and fluxes into the thin wave boundary layer. These sediment transport measurements were correlated with observed mean currents and rip channel evolution, and show a strong morphological response to the sediment flux.

14. SUBJECT TERMS sediment flux, sediment concentration, cross shore sediment transport, nearshore currents, acoustic backscatter, bistatic coherent doppler velocimeter (bcdv), scattering attenuation, nearshore canyon experiment (NCEX), bed echo, rip channel, Argus, variance image, pressure-velocity (puv) sensor, in situ calibration	15. NUMBER OF PAGES 75
	16. PRICE CODE

17. SECURITY CLASSIFICATION OF REPORT	18. SECURITY CLASSIFICATION OF THIS PAGE	19. SECURITY CLASSIFICATION OF ABSTRACT	20. LIMITATION OF ABSTRACT
Unclassified	Unclassified	Unclassified	UL

NSN 7540-01-280-5500 Standard Form 298 (Rev. 2-89)
Prescribed by ANSI Std. 239-18

THIS PAGE INTENTIONALLY LEFT BLANK

Approved for public release; distribution is unlimited.

USING ACOUSTIC BACKSCATTER TO MEASURE SEDIMENT FLUX IN THE SURF ZONE

Preston J. Roland
Lieutenant, United States Navy
B.A., University of Mississippi, 2000

Submitted in partial fulfillment of the
requirements for the degree of

MASTER OF SCIENCE IN PHYSICAL OCEANOGRAPHY

from the

NAVAL POSTGRADUATE SCHOOL
December 2006

Author: Preston J. Roland

Approved by: Timothy P. Stanton
Thesis Advisor

Edward B. Thornton
Second Reader

Mary L. Batteen
Chairman, Department of Oceanography

THIS PAGE INTENTIONALLY LEFT BLANK

ABSTRACT

Transport of sediment in coastal regions directly impacts mine countermeasure operations and naval construction efforts. Wave induced shear stress in the surf zone is responsible for entraining sediment particles into suspension within the combined wave and current boundary layer, where momentum is imparted through highly nonlinear processes. Therefore, a detailed understanding of sediment flux processes in the surf zone is essential to accurately model net sediment transport.

This study examines the use of acoustic backscatter inversion as a means of measuring sediment concentration profiles. Measurements of sediment concentration and velocity profiles were made by a high frequency Doppler velocity profiler deployed on Black's Beach during the Nearshore Canyon Experiment, NCEX. Profiles of sediment flux were compared with hourly mean current measurements from a cross-shore/long-shore array of PUV sensors and two-dimensional planner images of the morphological evolution provided by a three camera Argus video suite.

Observations from a seven day period containing the development and evolution of a weak rip channel demonstrated that acoustic backscatter inversion techniques, when calibrated with *in situ* sediment samples, provide high spatial and temporal resolution estimates of sediment concentration and fluxes into the thin wave boundary layer. These sediment transport measurements were correlated with observed mean currents and rip channel evolution, and show a strong morphological response to the sediment flux.

THIS PAGE INTENTIONALLY LEFT BLANK

TABLE OF CONTENTS

LIST OF FIGURES

THIS PAGE INTENTIONALLY LEFT BLANK

ACKNOWLEDGMENTS

Heartfelt gratitude is extended to those who forsake the throng and take the high road in an effort to improve our understanding of the world's last frontier. I would like to express specific thanks to my advisor, Dr. Timothy P. Stanton, whose work ethic, patience, determined instruction, and confidence were essential during the pursuit of this research. I have been pushed beyond what I thought was possible in order that my potential may be revealed. My growth as a scientist and naval officer is a direct result of your unrelenting commitment to excellence. I am also indebted to Mr. James Stockel and the other members of the Ocean Turbulence Research Group. Their assistance in all manner of technical endeavors has enabled the completion of this research.

Words can not capture the loving appreciation I wish to convey to my beautiful wife, Jennifer. You have the hardest job in the navy, and your enduring support is the hallmark of my success.

It is my deepest joy to acknowledge my creator and savior, Jesus Christ, whose hand has never left me. He is my rest, and with love and enduring faithfulness He sustains me.

THIS PAGE INTENTIONALLY LEFT BLANK

I. INTRODUCTION

During Operation Desert Storm, the USS Princeton was severely damaged by an Italian made Manta bottom-mine, immediately emphasizing the naval relevance of improving the fundamental understanding of sediment transport mechanisms for mine countermeasures. The emergent technologies such as synthetic aperture sonar and acoustic color imaging offer unprecedented capabilities in the detection of bottom mines, but are still subject to limitations associated with mine burial. To understand when scouring and burial conditions exist at a given site, it is critical to continue development of predictive models for sediment transport and morphological change in the nearshore. A detailed foreknowledge of the battlespace environment is essential to countering the asymmetric threats resultant in conducting power projection from the littoral.

In this study, detailed observations of suspended sediment concentration and three component velocity vector sediment flux are measured with a high resolution coherent Doppler profiler in order to determine the sediment flux in the context of comprehensive nearshore circulation measurements. The goal of this detailed boundary layer process study is to develop parameterizations for the measurement and modeling of wave and current-forced sediment transport in the inner shelf and surf zone.

A. THEORY OF SUSPENDED SEDIMENT TRANSPORT

The morphology of a natural beach is in a continuous state of change due to the constantly varying effects of waves and currents forced by wave breaking momentum transfer and winds. Forecasting these changes in beach structure with predictive models requires simplified models of the local sediment transport rate. Sediment transport rates are a function of the local wave energy and mean flow patterns, which in turn are determined by incoming waves interacting with existing topography, and prove complex to model accurately (Nielsen, 1992, p. 263). The following review will address the historical foundations of sediment transport modeling in the surf zone as an introduction to the direct, high resolution, field sediment transport profile observations used in this study.

Sediment transport within the surf zone occurs in two forms: bed-load sediment and suspended load sediment. Bed-load transport is regulated by intergranular forces occurring from particle-particle collisions or contact with sand grains resting upon the bed. Bed-load occurs in a very thin, high density layer at the bottom of the wave-forced oscillatory boundary layer. While bed-load is capable of significant sediment transport, it continues to be challenging to measure except in controlled laboratory experiments. Some fraction of the bed load is measured in the lower bins of the acoustic instrument used in this study. However, the very large sediment concentration limits acoustic penetration, and the finite bin size (1 cm) limits resolution of the bed load.

The suspended load is the sediment moving in suspension above the intergranular load layer by the vertical components of the turbulent velocity, arising from shear stress.

1. Entrainment of Bed Sediment

In order for transport to occur, sediment must be entrained from the bed into suspension and then momentum must be imparted on the suspended particles. Fluid motion interacts with the bed sediment primarily through shear stress, $\tau_o(t)$. In most models, the free stream velocity is scaled by a friction factor, f_w, to estimate the bed stress. Equation 1.1 is an example of a common model used to predict the peak bed shear stress under a sinusoidal wave, and may be applied to natural flows with an unmeasured local stress,

$$\hat{\tau} = \frac{1}{2}\rho f_w (A\omega)^2 \qquad (1.1)$$

where ρ is equal to the sediment density, A is the orbital amplitude of the fluid just above the boundary layer, and ω is the radian frequency $2\pi/T$ (Jonsson, 1966). Variability in parameterization of f_w is a major source of error for sediment transport models. Analysis of two empirical models for the wave friction factor has shown that the magnitude of f_w over flat sandy beds depends of the Reynolds number $A^2\omega/v$, while the magnitude of f_w over irregular beds is determined by the bed roughness r/A. The respective empirical models are shown by Equations 1.2 and 1.3, where v is the fluid viscosity and r is the hydraulic roughness (Kamphuis, 1975; and Justesen, 1988, cited in Nielsen, 1992).

$$fw = \frac{2}{\sqrt{\frac{A^2\ \omega}{\nu}}} \tag{1.2}$$

$$fw = \exp\left[5.213\left(\frac{r}{A}\right)^{.194} - 5.977\right] \tag{1.3}$$

Determining the bed shear stress τ is necessary to calculate the Shields parameter θ, which is a measure of the balance between disturbing forces and stabilizing forces that act on the bed sediment. The Shields parameter scales with the total bed stress, and for sinusoidal wave forcing it is usually expressed in terms of peak bed shear stress,

$$\theta = \frac{\widehat{\tau}}{\rho(s-1)\,g\,d} = \frac{\frac{1}{2}\ f_w\,(A\omega)^2}{(s-1)\,g\,d} \tag{1.4}$$

The entraining forces in Equation 1.4 are in the numerator, while the stabilizing forces due to gravity *g*, the relative density of the sediment *s* and the sediment grain diameter *d*, are in the denominator (Shields, 1936, cited in Nielsen, 1992). The Shields parameter can be further modified to reflect the important role of bedforms and sediment characteristics, by considering the separate contributions of the skin friction and form drag, acting on the surface grains of sediment resting along the bed.

The effective Shields parameter at which sediment movement occurs is known as the critical Shields parameter θ_c. An empirical analysis determined that for typical beach sand with a diameter of 0.2 mm and a relative density of 2.65, the overall value of $\theta_c \approx 0.05$ (Nielsen, 1992, pp.103-107). A result of the sudden initiation of sediment associated with forcing above θ_c is that sediment entrainment and transport is a highly nonlinear process dependent on the total mean current and wave induced stress imparted on the bed.

2. Cross-Shore Movement of Sediment in Suspension

Sediment transport requires bed shear stress and current velocity profiles under combined wave and current conditions in order to be modeled (Liu, 2001). Once sediment has been suspended from the bed by the stress associated with wave and current friction, sediment is entrained into the bottom wave and low frequency boundary layer where momentum is imparted by the nearshore low frequency currents and mean wave motions (Figure 1).

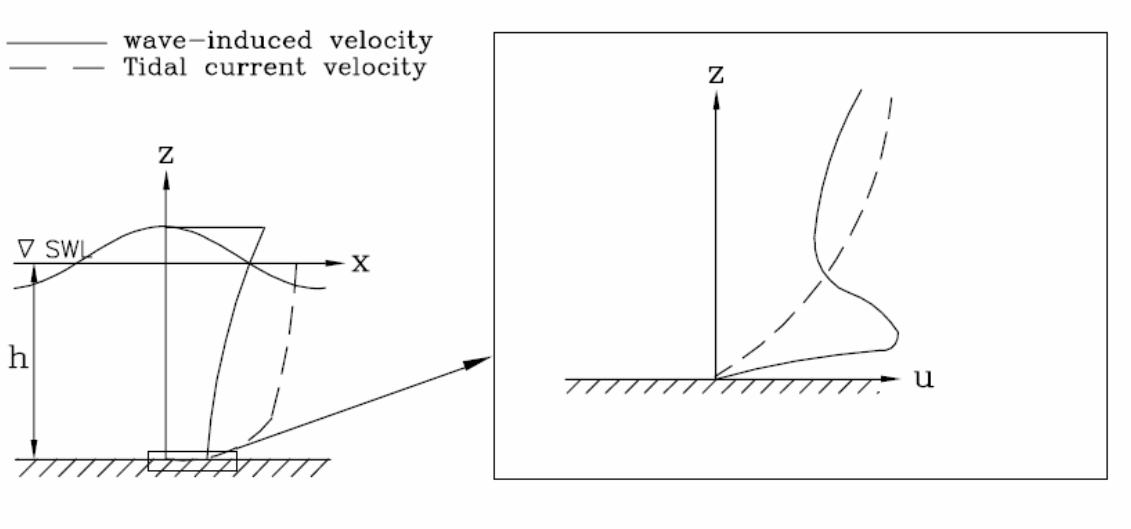

Figure 1. Comparison of relationship between tidal current and wave induced velocity profiles for the thin bottom boundary layer found over flat, sandy beaches (Liu, 2001). Even though the mean current velocity boundary layer dominates most of the water column, the highly sheared wave-induced boundary layer just above the bed is the primary suspension and transport mechanism near the bottom. Predictive modeling of sediment transport in the surf zone requires parameterization of the temporal and spatial relationship between the mean current and wave-induced boundary layer.

Sediment flux is the amount of sediment mass transported through a unit of length per unit of time. In order to parameterize sediment flux, the majority of sediment transport models use the product of a time-averaged sediment concentration and the time-averaged velocity components as they vary in depth (Equation 1.5) where $u = (u, v, w)$ (Nielsen, 1992, p. 264).

$$\overline{Q} = \overline{c} * \overline{u} \tag{1.5}$$

Due to the nonlinearity of the suspension process, this approach is subject to large errors. An alternative modeling technique, based on the product of the instantaneous sediment concentration and the instantaneous particle trajectories, incorporates the Shields parameter into a pick-up function p(t) that is designed to parameterize the entrainment processes at the bed, as opposed to the bulk sediment concentration. The subsequent momentum of the suspended sediment is explained by the jump length l_x(t), which is the distance traveled by each particle per unit time, as described in Equation 1.6 (Nielsen, 1992, p. 265).

$$Q(t) = p(t) * l_x(t) \tag{1.6}$$

In this study direct observations of current profiles and suspended sediment were made during a nearshore field experiment. The Bistatic Coherent Doppler Velocimeter (BCDV) is a high resolution acoustic Doppler backscatter instrument developed by the Ocean Turbulence Laboratory at the Naval Postgraduate School. The BCDV is utilized in this study and directly calculates lateral sediment flux profiles through the product of the instantaneous velocity and sediment concentration. This allows comparison with models of suspension and transport. Equation 1.7 directly calculates the instantaneous cross-shore sediment flux as functions of the height above the bed.

$$Q(t,z) = c(t,z) * \vec{v}(t,z) \tag{1.7}$$

One advantage of this method of sediment flux measurement is that it does not require perfect knowledge of τ_o, which is challenging to estimate in cases of irregular flow. Additionally, the detailed mean current and wave-induced boundary layers are directly measured by the BCDV, therefore allowing the parameterization required for modeling sediment transport. The BCDV is discussed further in Section II.C.

B. ACOUSTIC MEASUREMENT OF SEDIMENT CONCENTRATION

Acoustic backscatter measurement of sediment concentration has been validated by various experiments over the last two decades and has the advantages of being non-intrusive, providing a complete profile, and offering higher temporal and spatial resolution than other sampling methods. Backscatter profiling is the process in which the

transducer of an acoustic measurement device transmits high frequency acoustic energy that generates a narrow insonified volume through the water column. The acoustic beam width and transmit duration define the sample volume, and suspended particles reflect acoustic energy back toward the transducer where it is measured as a function of range. Acoustical systems must infer the suspended sediment concentration from an inversion of the returned backscatter profile.

There are two challenges in inferring suspended sediment concentrations from these backscatter profiles. The first stems from the fact that the inversion algorithm applied to the acoustic pressure variance returned by acoustic Doppler is a non-explicit solution since the scattering/attenuation due to suspended sediment in the water column is itself a function of the unknown mass concentration profile. Piecewise integration techniques are used in this study (Section II.C.3). The other limiting factor pertains to the presence of air bubbles within the water column. Injected from breaking waves at the surface, air bubbles produce large backscatter returns that inhibit the accurate measurement of suspended sediment, and these bubble scatterers are not distinguishable from the suspended sediment backscatter.

C. SCOPE OF RESEARCH

Building upon the work done in development of the Coherent Acoustic Sediment Probe, this research is focused on processing field measurements from the BCDV during the Nearshore Canyon Experiment. Suspended sediment and sediment flux are measured with the BCDV high-resolution coherent Doppler to estimate the three-component velocity vector, sediment concentration, and resulting fluxes. Laboratory measurements are used to validate calibration techniques based on in situ sampling as well as to evaluate algorithms designed to limit inversion errors and include compensation for the presence of air bubbles in the profile.

The Office of Naval Research has identified the ability to observe, measure, and predict small and large scale processes in the surf zone as essential to the success of future naval operations. The primary goal of this research is the application of a proven acoustic backscatter inversion technique to a data set collected during a nearshore

experiment, with the objective of comparing the resultant current velocity and sediment concentration profiles with existing models.

There are two major nearshore processes used in modeling the cross-shore movement of sediment, both related to the breaking of waves as they shoal in the surf zone. Nonlinear wave motions force net sediment movement as the result of asymmetries resulting from the steepening and breaking of wave oscillatory motion as they shoal. Cross-shore currents are driven by the momentum flux imparted by the radiation stress of breaking waves and are pervasive, constantly creating change on morphological structures while simultaneously being influenced by the flow around those same structures.

THIS PAGE INTENTIONALLY LEFT BLANK

II. EXPERIMENT

A. NCEX BACKGROUND AND SET UP

Many continental selves have abrupt, irregular bathymetric features that cause large gradients in the wave field outside the surf zone, yet few studies have been conducted as to how these dynamic environments impact the underling physics utilized by nearshore models. The Nearshore Canyon Experiment (NCEX) makes use of extreme topographic phenomena near La Jolla, California in order to host experiments designed to evaluate the affects of abrupt coastal bathymetry on nearshore processes (Figure 2).

A research team from the Naval Postgraduate School's Nearshore and Ocean Turbulence labs participated in NCEX during September through December 2003 with the goal of obtaining detailed measurements of the effects of steep topography on incident swell, wave shoaling, inner shelf currents, and sediment transport on a narrow continental self. At the northern end of the NCEX field site, near Black's Beach, a directional wave buoy, two RDI acoustic Doppler current profilers, and both a cross-shore and long-shore array of digital electromagnetic pressure-velocity (PUV) sensors were deployed (Figure 3 and Figure 4). Several of the PUV instrument sites also included high resolution pressure transducers to resolve low frequency pressure gradients. A high resolution bottom boundary layer instrument suite used in this study was deployed at the intersection of the longshore/cross-shore arrays.

B. ENVIRONMENT

1. Field Site Bathymetry

The heads of both the Scripps and La Jolla submarine canyons are located within a few hundred meters of shore at the NCEX field site near La Jolla, California. The dramatic changes in wave energy associated with the canyons' proximity to the beach occur over a relatively short alongshore distance and produce complex nearshore circulation and morphological transformations (http://science.whoi.edu/users/elgar/NCEX/ncex.html). Rapid changes in morphology were observed throughout the experiment and are discussed in more detail in section III.B.

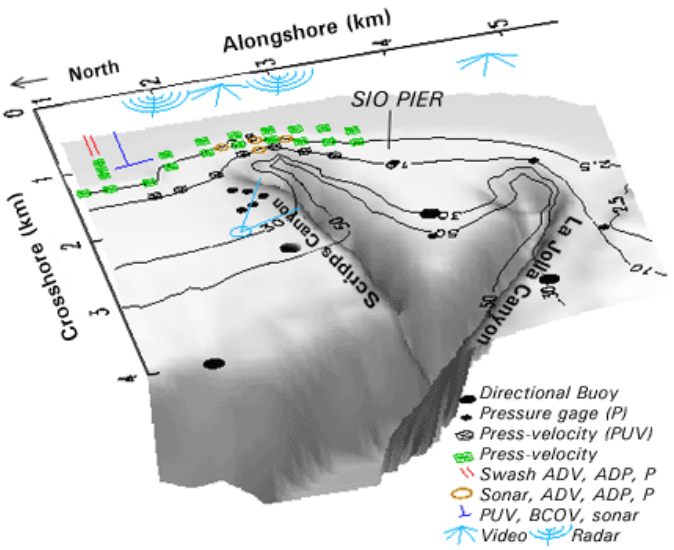

Figure 2. Overview of instrument locations at the NCEX field site (http://science.whoi.edu/users/elgar/ NCEX/ncex.html).

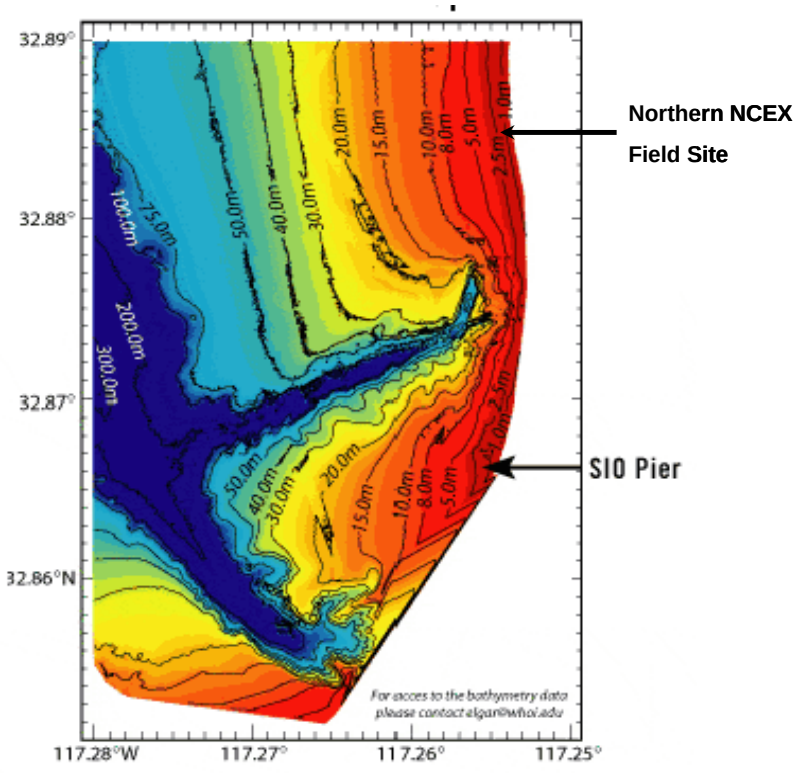

Figure 3. Bathymetry of the Scripps and La Jolla canyons at the NCEX field site (http://science.whoi.edu/users/elgar/ NCEX/ncex.html).

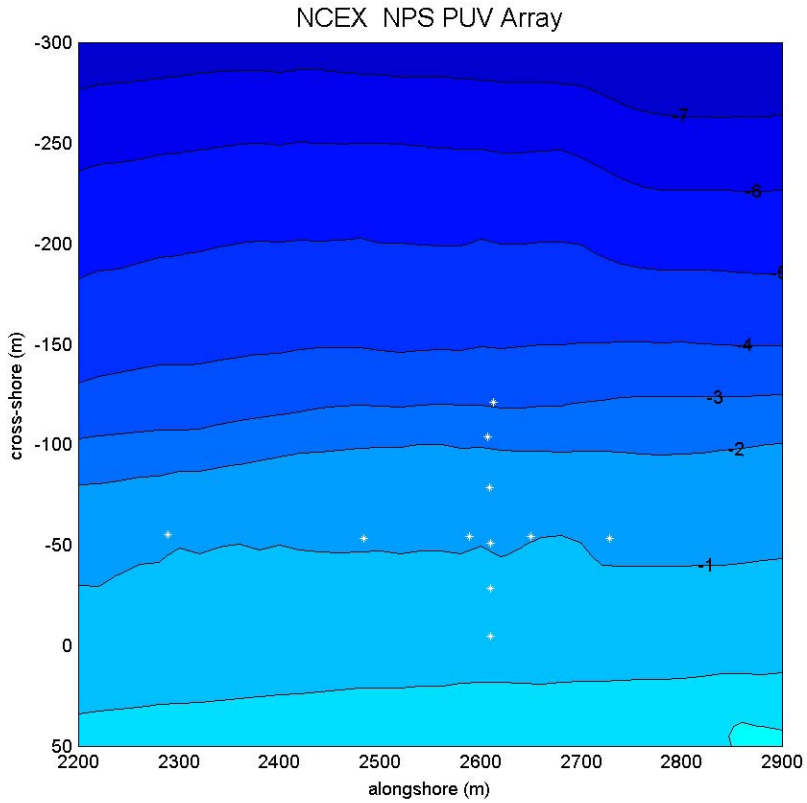

Figure 4. Location of NPS instruments (white) across the surf zone at the northern NCEX field site. The bottom boundary layer instrument suite, including the BCDV, is located at intersection of the cross-shore / long-shore PUV sensor array. Bathymetry was measured every four days by a jet ski equipped with a differential Global Positioning System.

An Argus video beach monitoring system was used to view the bathymetry within the surf zone. Developed by the Coastal Imaging Laboratory at Oregon State University, Argus utilizes multiple high resolution cameras and video remote sensing techniques in order to provide a time series of geo-referenced digital pictures of wave breaking patterns (Holman). Rectified brightness variance images, which display the pixel-to-pixel variation in light intensity during a 10 minute period, separating the dynamic from the steady state areas of the image, proved particularly useful in determining the distribution of waves breaking in the surf zone. Bright areas of the images represent wave braking due to shoaling associated with shallow depths, indicating the shallow depths of the bar. The dark areas of the variance images have negligible wave breaking, indicating deeper water or areas inshore of the surf zone. Trough channels are seen as darker swaths

running parallel to the shore in between the lighter lines associated with sand bars. The time series inputs from three cameras mounted at the NOAA building located on the cliffs above Black's Beach were combined and rectified onto a map plane in (x, y) coordinates in order to provide maps of wave breaking patterns that spanned the experiment site. The mean surf zone width was 115 meters throughout the course of the experiment. Waves within the surf zone are characterized as spelling rather than plunging breakers, due to the low slope of the broad sandy beach. Since wave breaking in shoaling conditions is directly modulated by the mean water depth, the areas of breaking waves reveal the spatial structure of the nearshore morphology.

Although bathymetry was directly measured by a jet ski equipped with a differential GPS every four days, Argus brightness variance images were useful in interpreting the bottom boundary layer measurements made by the BCDV, as they showed the cross-shore position of these measurements within the surf zone, and changes in morphological structure with high temporal resolution. For example, in Figure 35, the position of bars and the cross-shore rip channels are clearly seen in the variance mean pixel images.

Ocean waves carry with them a flux of momentum expressed as a radiation stress. As waves break, the radiation stress cross-shore gradient is diffused and the momentum is transferred into the water column, forcing nearshore currents. This generation of low frequency currents in the surf zone is an important mechanism in net sediment transport. The time sequence of location and shape of the sand bars and rip channels within the surf zone provide insight into the morphological evolution at the boundary layer measurement site. Nearshore circulation was directly measured at each location in the high resolution cross-shore/long-shore PUV sensor arrays.

2. Sediment Measurements

Sediment samples were collected over the course of 16 days from locations within 30 m of where the bottom boundary layer instrument suite was mounted. These samples were used to calibrate the backscatter response of the BCDV and exhibited similar

unimodal profiles, indicating that most of the beach near the instrument frame had a uniform sediment composition with 0.18 mm mode diameter (Figure 5).

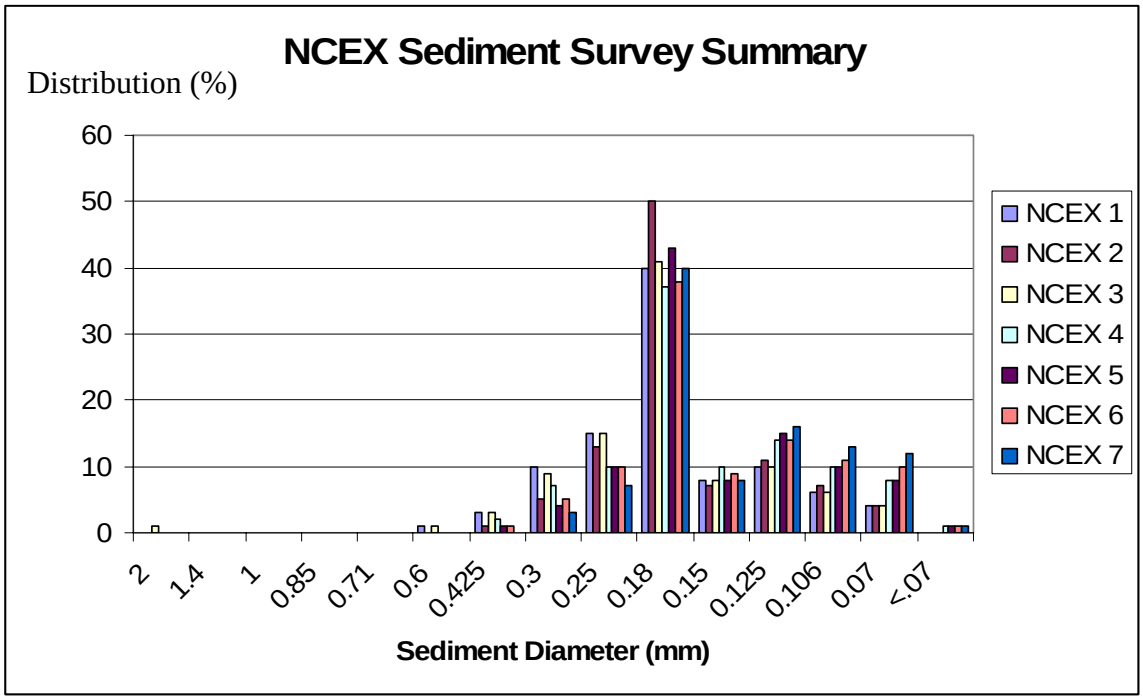

Figure 5. Size distributions for seven sediment samples collected during NCEX. The profile is unimodal, indicating that most of the beach near the instrument frame had a uniform sediment composition with 0.18 mm mode diameter.

3. Wave Measurements

Data on the offshore wave conditions during NCEX was provided by a Datawell directional wave buoy moored at a depth of 32 meters directly in line with the other instruments of the cross-shore array. Time series of significant wave height, peak period, and propagation direction were generated and used in the analysis of the surf zone observations. The size and direction of offshore waves determine their breaking characteristics as they shoal within the surf zone, as larger amplitude waves will break in deeper water than similar waves of smaller amplitude, changing the breaker location as measured in the Argus variance maps. Larger waves transfer increased momentum and energy to the surf zone as they break resulting in increased bed shear stress $\tau_o(t)$ and enhanced low frequency currents.

C. BCDV AND PROCESSING

1. BCDV

The Bistatic Coherent Doppler Velocimeter (BCDV) was developed by the Ocean Turbulence Research Group at the Naval Postgraduate School to measure three-component velocity and sediment concentration in 1cm bins at 16 Hz over a 1 m range above the bed (Figure 6) (Weltmer, 2003). During NCEX, this instrument was mounted on an H-frame (Figure 7) within the surf zone. It uses a single monostatic transducer to emit acoustic pulses at 1.25 MHz, then receives backscattered energy at the central transducer and the 3 surrounding bistatic transducers at 1cm range bins out to 1.2 m range. The BCDV is unique in that it can directly measure the instantaneous velocity vector and sediment concentration through the water column (Stanton 1996, 2006).

For NCEX, the BCDV was deployed as part of a high resolution bottom boundary layer instrument suite designed to directly measure velocity and sediment concentration and bedforms in the surf zone in order study nearshore sediment transport processes and refine their parameterization of models. The face of the monostatic transducer was mounted approximately 1 m from the seabed, looking down. Sediment concentration profiles were estimated from an inversion of the backscattered acoustic intensity measured by the central transducer over an 80 dB dynamic range. A laboratory calibration, based on *in situ* sediment samples collected during the experiment, was conducted and is discussed in the following section.

In order to see boundary layer properties at the time series of wave groups, 16 Hz velocity, sediment concentration, and sediment flux profile observations were averaged over 2 minutes. The 60 minute mean of these averaged observations was then utilized to generate profiles of cross-shore/long-shore velocity and sediment flux.

Figure 6. Bistatic Coherent Doppler Velocimeter (BCDV) developed at NPS by Dr. T.P. Stanton and the Ocean Turbulence Research Group. The BCDV directly measures instantaneous sediment concentration and velocity through 1 m of water with 1 cm resolution.

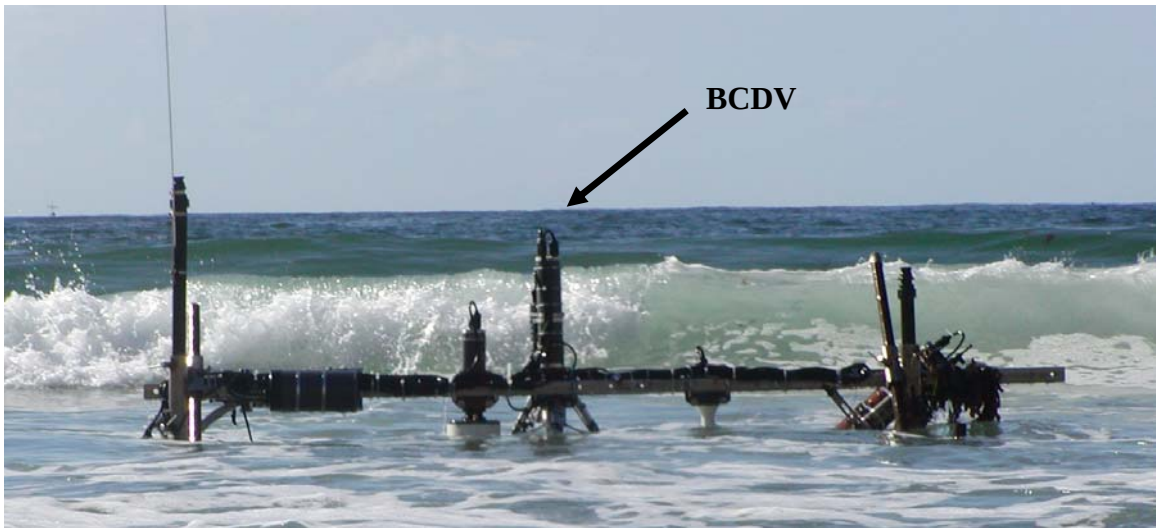

Figure 7. Bottom Boundary Layer instrument frame located at the intersection of the NPS cross-shore and long-shore instrument array. The BCDV current and sediment profiler is located near the middle of the frame.

2. Wave Forcing Measurements

The BCDV measures three-component velocity profiles at 16 Hz (Figure 8). The wave asymmetry, determined by the skewness and kurtosis of the profiles, indicates the amount of cross-shore forcing that occurs when the oscillatory motion of the waves break down as a result of shoaling. This technique is demonstrated in the cross-shore velocity time series (Figure 8, top panel), which show the sharp, narrow peaks near 25 s that indicate the presence of onshore wave forcing due to bores. The rapid change in the velocity gradient with respect to depth *z* is associated with the wave induced boundary layer and indicate intense the shear stress. In contrast, the vertical velocity (Figure 8, bottom panel) changes linearly with respect to depth. The 60 minute means of the skewness and kurtosis profiles, depicted in Figure 9, were used to evaluate onshore wave forcing during NCEX.

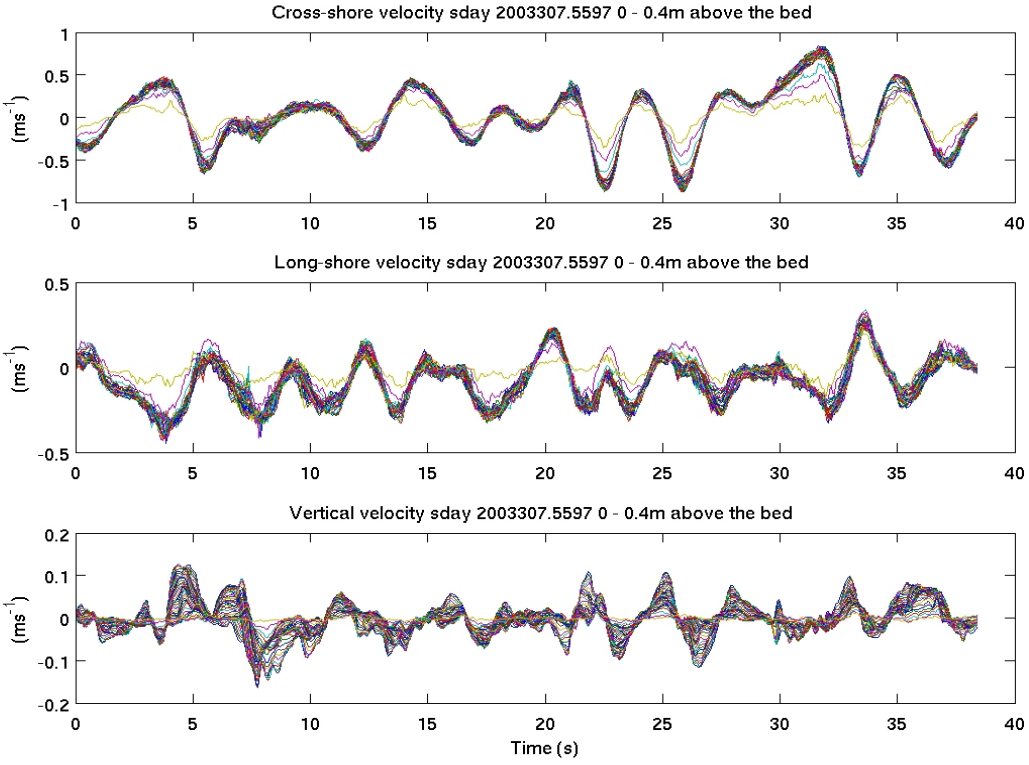

Figure 8. 16 Hz sampled velocity (u, v, x) time series recorded by BCDV for bins in the bottom 40 cm above the bed. Each time series is a 35 s time series of the instantaneous velocity returned at 1 cm resolution. Strong gradients in the cross and long shore components are seen in the bottom 2-4 cm, spanning the thin oscillatory boundary layer in the flat, sheet-flow environment seen below the BCDV.

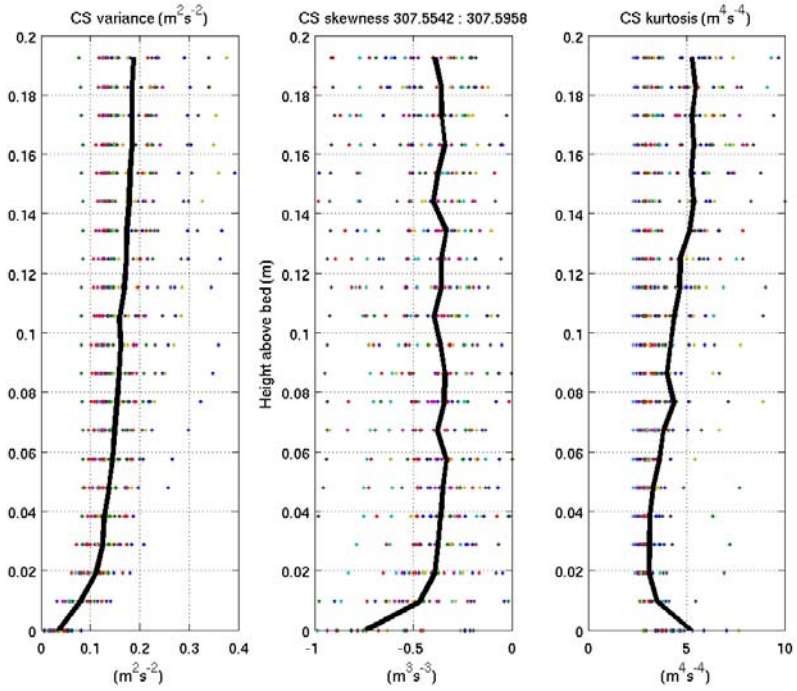

Figure 9. Profiles of hourly mean of cross-shore variance, skewness, and kurtosis. Each point represents a 2 minute average of the 16 Hz sampled variables, capturing variability at wave group periods.

3. Backscatter Calibration

The concentration of suspended sediment is inferred at each BCDV time interval from an inversion of the profile of backscattered acoustic energy. The inversion relationship between returned acoustic energy and sediment concentration is expressed by Equations (2.1) and (2.2),

$$C^2(r) = \left(\frac{k_s\, k_t}{\psi\, r} \right)^2 \; M\; e^{4(\alpha_s + \alpha_w(M))} \tag{2.1}$$

$$M(r) = \left(\frac{C\; \psi\; r}{k_s\, k_t\, r_o} \right)^2 e^{4r(\alpha_w + \alpha_s(M))} \tag{2.2}$$

where C is the root mean square of the digitized count level averaged at the 16 Hz output rate that represents the acoustic amplitude received by the transducer of the BCDV, M is the mass of the suspended sediment in grams per liter, r is the range from the transducer face to the range bin being sampled, k_s contains the sediment specific information (form function, particle size, and sediment density), k_t contains the system specific parameters (pressure at r_o, pulse duration, sound velocity, wave number, directivity Bessel function, transceiver radius, and subtended angle to the acoustic axis), and Ψ accounts for the departure of the backscattered signal from spherical spreading in the transceiver near field (Thorne, 1995). The total acoustic attenuation term, α, is comprised of terms for the scattering attenuation α_s due to the presence of suspended sediment $M(r)$ and the attenuation due to absorption in clear water, α_w.

As detailed by Clay and Medwin (1977), α_w can be determined based on the physical characteristics of water and has a value of 0.316 dBm^{-1} for seawater at 14° C. Since calculation of the total attenuation term $\alpha(M)$, however, requires knowledge of the sediment concentration, which is the unknown quantity sought, Equation (2.2) does not have an explicit solution. Therefore a piecewise integration technique is applied to the backscatter inversion in order to infer the sediment concentration from backscatter intensity.

Potential sources of error associated with the piecewise integration technique exist due to the complexity and inaccuracy of models for terms α_s and k_s. This study utilizes laboratory calibrations based on in situ samples collected from the field site during the experiment in order to produce calibration coefficients that will eliminate these potential sources of error. This direct calibration has the advantage of requiring no a priori assumptions about the sediment spectra and backscatter system response (Stanton, 1996). A test tank was constructed using a 600 gallon acrylic aquarium equipped with a computer-controlled X/Y positioning stage, from which the BCVD is suspended. An internal test vessel designed to contain a known concentration of well mixed sediment samples is placed within the test tank. The BCDV acoustic beams are directed through a thin plastic film window in the side of the acrylic test vessel which contains water and carefully measured masses of test sediment, while a strong impeller-driven pump rapidly

circulates the fluid and sediment within the measured volume of the vessel, creating a well homogenized volume with known concentration. As the test volume and sediment mass are known, the backscatter level to concentration relationship for all the beams can be readily determined (Stanton, 1996).

a. Attenuation Calibration

Attenuation present in the water column will cause a decrease in the intensity of acoustic backscatter as it travels through the insonified beam. In the nearfield, air bubbles entrained by rolling breakers are always present in the upper water column of the surf zone and therefore sediment concentrations obtained from the inversion of the backscatter will consistently be underestimated. In the bottom boundary layer, the large concentration of sediment causes strong scattering. A value for scattering attenuation term α_s is estimated by a linear fit to the exponential decay of the signal response across the signal volume, with the radial spreading term removed (Stanton, 1996). The attenuation calibration coefficient for each concentration mass level, $\alpha_s(M)$, is regressed between α_s and the known concentration mass levels. This process ensures that the attenuation is a function of the scattering cross section of the sediments at the working frequency.

b. Sediment Mass Calibration

The sediment mass calibration coefficient, *calmass*, is determined by a linear fit between the received power C^2 and the known sediment mass concentration (Stanton, 1996). The range-dependent radial spreading term and integrated attenuation coefficients are applied across the sample volume in order to remove the range-dependent attenuation effects.

4. Application of Mass and Attenuation Calibration Coefficients to Determine Suspended Sediment Concentration

The above laboratory-derived attenuation and mass calibration coefficients are used to convert profiles of backscattered acoustic energy to mass concentration profiles using a piecewise integration inversion of the returned acoustic backscatter.

$$M(r) = \frac{(r)^2}{(r_o)^2} * calmass * C^2(r) * e^{4\int_0^r (\alpha_w + \alpha_s(M))\, dr} \qquad (2.3)$$

where C^2 is the digitized acoustic pressure level squared, *calmass* is the sediment calibration coefficient, r_o is the range at which calmass was measured and $(r/r_o)^2$ is the radial spreading compensation term (Stanton, 1996). The calibration coefficients *calmass* and α_s integrate specific backscatter characteristics of the observed sediment into the acoustic model.

Starting with the first range bin of the radial spreading corrected backscatter profile, the mass calibration coefficient, *calmass*, is applied to the returned backscatter in order to estimate the sediment concentration of the first bin $M(1)$. $\alpha_s(1)$ is then estimated using $M(1)$, so the total attenuation due to water α_w and scatters $\alpha_s(1)$ is estimated for the first bin. This attenuation is then piecewise integrated to the following bins.

A source of error associated with this technique is the presence of bubbles within the insonified nearfield region of the transducer. This region composes eight or nine bins at the top of the sample range that is not measured. Subsequently, the scattering attenuation caused by the bubbles in these blanked bins can not be directly measured. In order to limit this potential error, an exponential fit to the known concentration profile is extended to the blanked bins.

Since the effects caused by attenuation are less prevalent when sediment concentrations are low and will become significant as concentrations increase, this algorithm has been checked by applying it to known sediment concentrations used with the original tank backscatter calibration of the BCDV. The calibration runs were conducted with sediment samples taken from the NCEX field site during the experiment. For NCEX nine concentrations spanning 0.0144 to 12.804 gl^{-1} were measured. Plots of

sediment concentration vs. range bins corresponding to the calibration runs are shown in Figure 10 through Figure 15 and show the known sediment concentration level (green), sediment concentration determined by an inversion of returned backscatter with no attenuation terms applied (blue *), and sediment concentration determined by an inversion of returned backscatter with α applied (red).

Runs 1 and 2 were conducted with no sediment in order to get a baseline for the test vessel in both the undisturbed and stirred modes. Runs 3 through 7 had sediment concentrations of less than one gram per liter. These runs demonstrate that the sediment concentration profile returned by an inversion of the backscatter is not significantly affected by the piecewise integration of the scattered attenuation $\alpha_s(M)$ (Figure 10 and Figure 11) for low levels of sediment concentration. The initial spike in suspended sediment concentration at range bin 64 is a response from the thin plastic acoustic window of the test vessel and is present in all calibration profiles, and accounted for in the calibration.

Runs 8 through 10 were conducted with sediment concentration levels of 1.26, 2.71, and 5.59 gl^{-1} respectively. Sediment concentration profiles returned show a uniform profile shape, yet the calibration of returned backscatter with no attenuation terms applied shows an apparent decrease of concentration across the test volume (Figures 12, 13, and 14). The backscatter variability within the test volume is thought to be due to multiple reflections of acoustic energy returning from the back of the acrylic test vessel, located at range bin 86.

At higher concentrations, such as those found in the saltation events near the bed, applying the calibration coefficient to the inversion is essential to extracting an accurate sediment concentration profile, as illustrated by run 11 (Figure 15). At a sediment concentration level of 12.8 gl^{-1}, the inversion with no attenuation terms applied generated a sediment profile that was several gl^{-1} below the known concentration in the well mixed test volume, demonstrating the ability of the piecewise integrated attenuation algorithm to measure sediment concentration profiles to concentrations well in excess of 10 gl^{-1}.

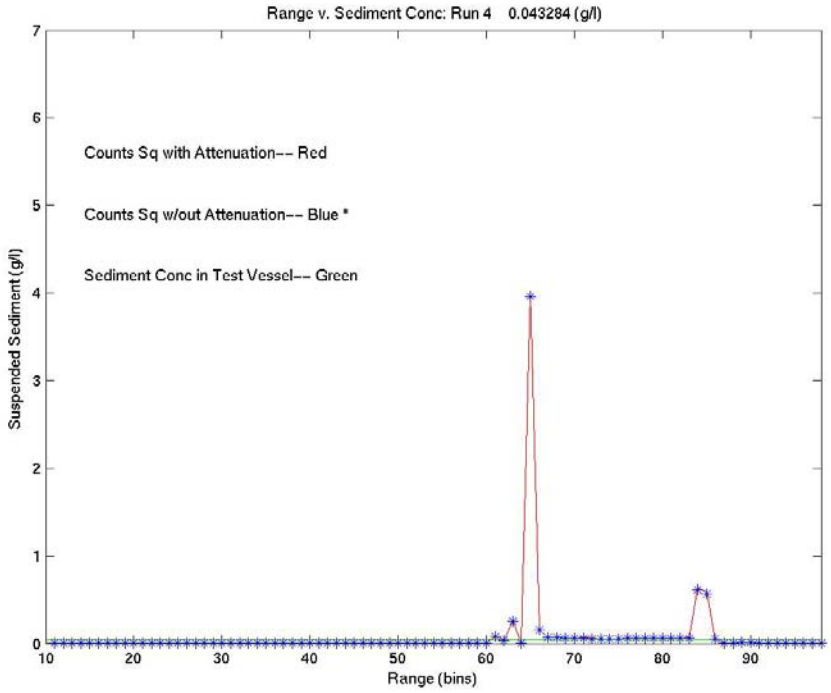

Figure 10. Concentration profiles with /without applied Attenuation Calibration: Run 4.

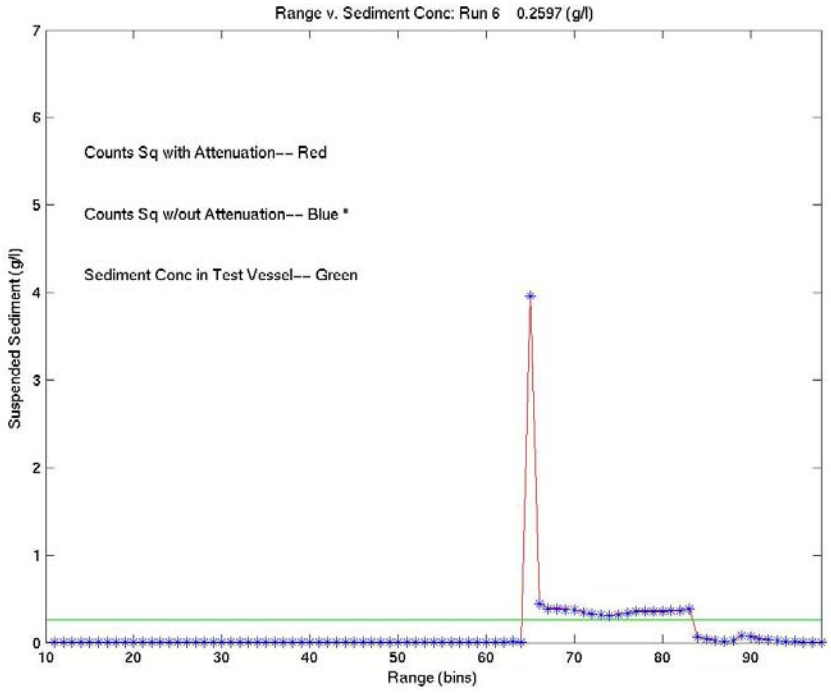

Figure 11. Concentration profiles with /without applied Attenuation Calibration: Run 6.

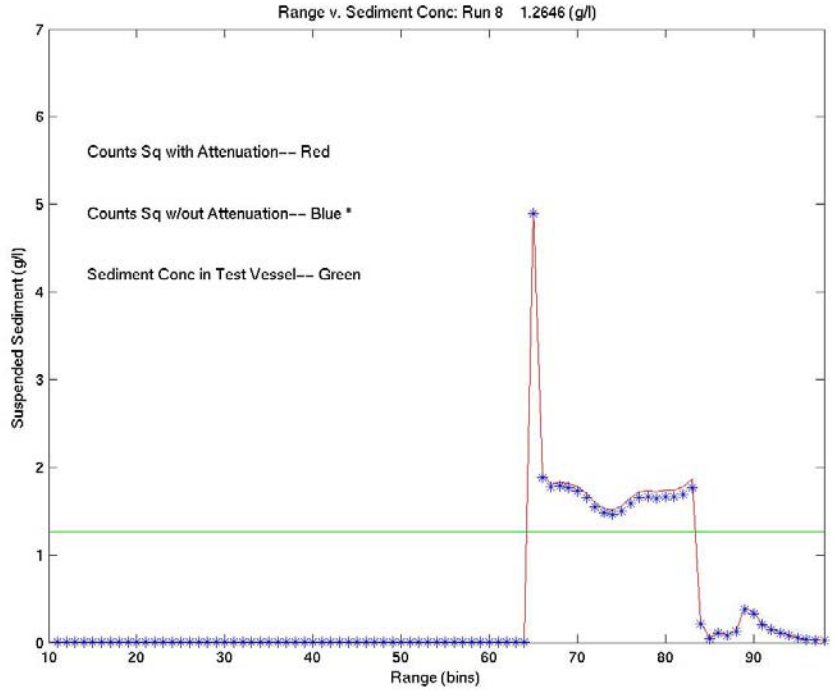

Figure 12. Concentration profiles with /without applied Attenuation Calibration: Run 8.

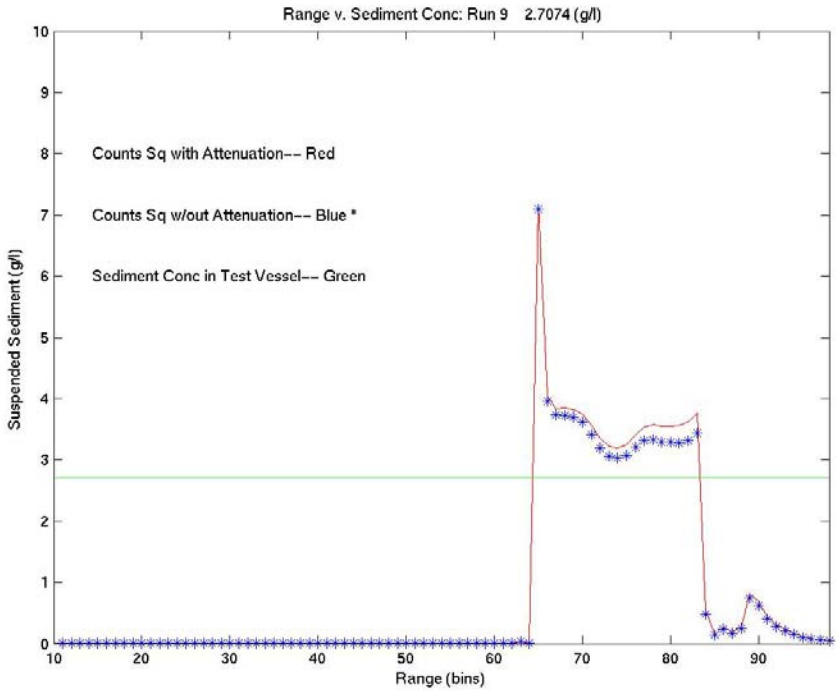

Figure 13. Concentration profiles with /without applied Attenuation Calibration: Run 9.

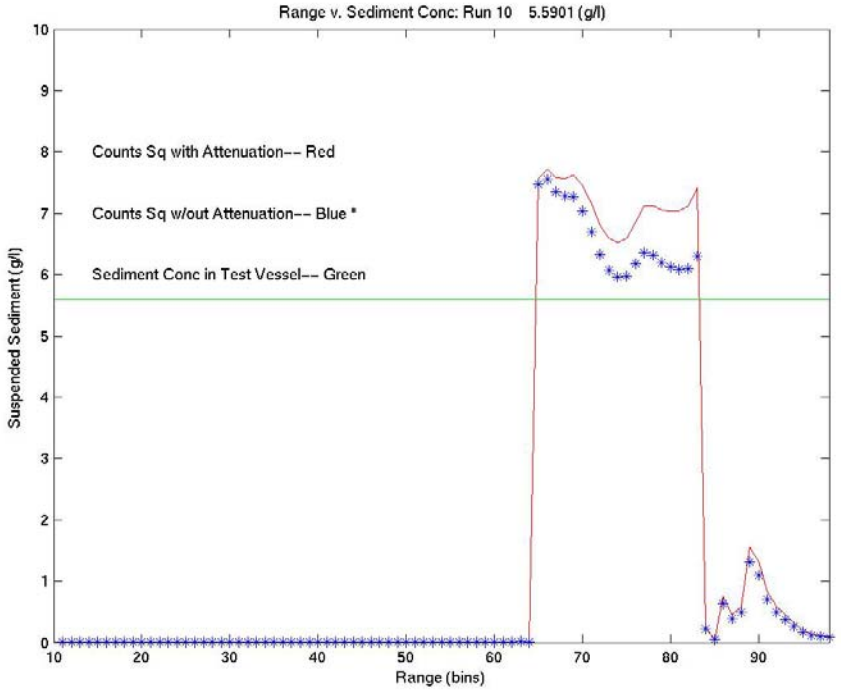

Figure 14. Concentration profiles with /without applied Attenuation Calibration: Run 10.

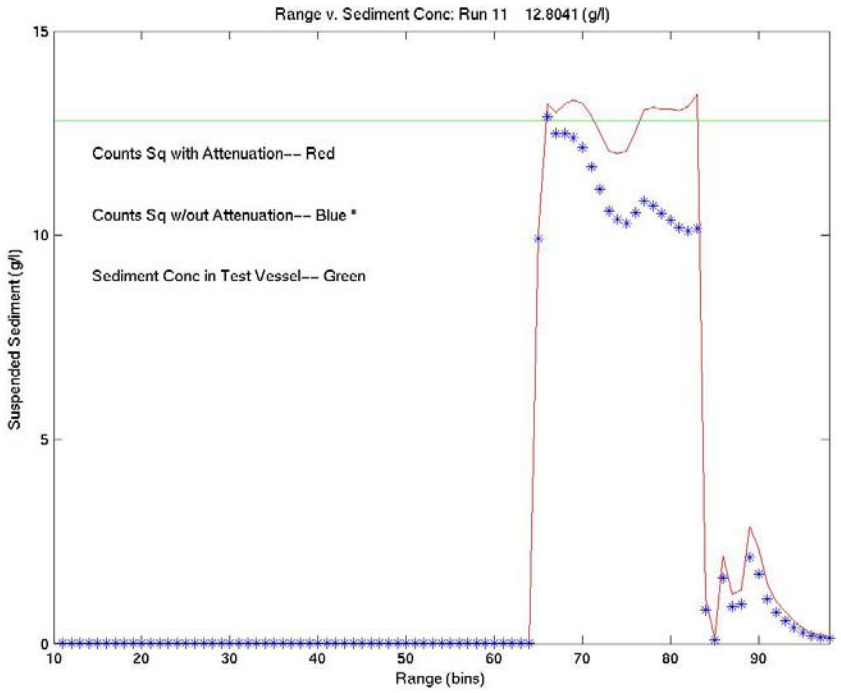

Figure 15. Concentration profiles with /without applied Attenuation Calibration: Run 11.

5. Use of Bed Echo to Constrain Error

a. Theory

Measurement of suspended sediment concentrations through the inversion of acoustic backscatter is susceptible to errors stemming from intrinsic variance in estimates of along beam attenuation due to scatterers along the beam. The use of acoustic echo return from the bed was considered as a means of constraining errors in the sediment concentration profile. The underling theory is that the amplitude of the bed echo should be constant, and can be used to constrain the piecewise integration of attenuation (e.g. Thorne, 1995). However, under wave forced saltating (suspending) conditions, the scattered echo from the seabed is not constant as the scatterer elements move through the insonified volume. This study explored the validity of this bed scatter constraint as well as the possible correlations between sediment concentration in the nearfield and bed echo.

b. Evaluation

The use of bed echo as means of evaluating sediment concentration profiles was ultimately not pursed in this research. The problem with this technique is related to fact that bed morphology is always in a state of change, and even small variances in the granular structure of the bed have a significant effect on the returned echo. As shown in Figure 16, at the high frequencies (1.25 MHz) used by the BCDV, the granular bed (0.2 mm) is a diffuse reflector whose net reflection is dependent on the arrangement of scatters within the insonified area. Variability in the intensity of the bed echo is also introduced due to the changing slope of ripples and other bedforms along the bed. Thorne (1995) proposed that the amplitude of the bed echo, averaged over 1 and 10 minute intervals, could produce a constant amplitude value and account for changes in the bedforms. This technique, however, does not represent a robust means of constraining the sediment concentration profile at the sample rate of the BCDV (15 Hz update rate) which resolves turbulence and wave motions.

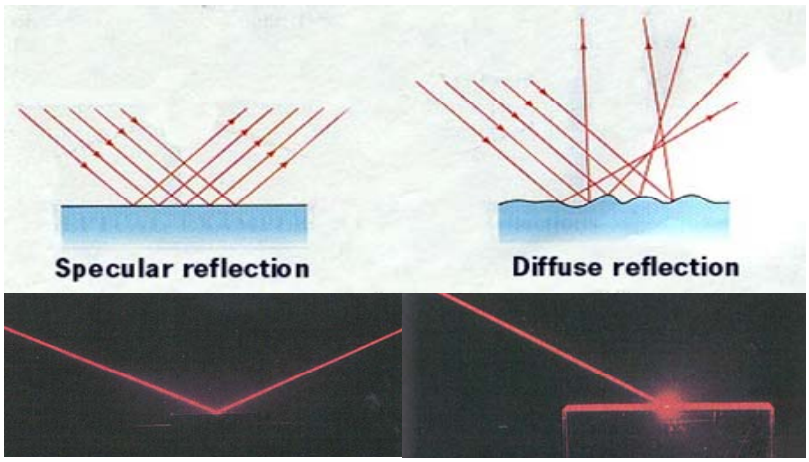

Figure 16. Specular v. Diffuse reflection (Hewitt, 1985). Diffuse reflection is more characteristic of the seabed, where scatterers on the granular scale and ripples prevent a uniform return of acoustic energy.

A further reason that bed echo was not utilized in constraining the sediment concentration profiles is related to the way in which the BCDV initially processes data. In order to reject acoustic sidelobe contributions from fixed structures, the Doppler processing is designed to ensure the maximum sensitivity is given to sediment that is in motion, so the BCDV rejects echo returns without Doppler shifts. This technique prevents the acoustic reflection from stationary objects, such as the bed, from obscuring the particles of interest that are in transport. Having rejected bed echo as means of constraining error, additional criteria for assessing the quality of the sediment concentration profiles must be implemented in order to ensure the accuracy of $M(z,t)$ measurements.

D. CRITERIA FOR EVALUATING DATA RETURNED BY BCDV

A major source of error in the acoustic measurement of suspended sediment is attenuation due to scatterers in the upper water column, near the central transmitter transducer. In this study these scatterers consist of air bubbles entrained during wave breaking that become suspended in proximity of the instruments nearfield, causing substantial attenuation along the insonified volume. This attenuation causes errors in the attenuation profile estimates that are carried forward by the piecewise inversion of the backscatter that is used in the determination of sediment concentration. In extreme cases,

it is so severe that it shadows the water column and masks the presence of the bed return and dramatically reduces the pulse-to-pulse coherence measured in the doppler velocity processing.

Another potential source of error in surf zone observations is the air-ocean interface that prevents acoustic measurement when the transducer face is out of the water. Placement of the H-frame instrument mount within a dynamic surf zone increases exposure to both the attenuation due to the presence of bubbles as well as to dropouts during lower tidal conditions.

In this study errors are constrained by evaluating BCDV returns via a joint condition that requires that the transducers are submerged and a prescribed coherence level is maintained through the profile. Once evaluated, only the non-corrupted observations are utilized to determine sediment flux and mean currents.

The following criteria were adopted:

1. Pressure Criteria

A mean of the pressure returned by the BCDV allows the overall quality of data to be evaluated by determining when the face of the BCDV transducer is out of the water during a tidal cycle. Additionally, a consistently high pressure over the transducer indicates that waves are breaking above, as opposed to on, the transducer. Air bubbles entrained by waves breaking a greater distance above the transducer will not propagate as far into the insonified sample volume, causing less attenuation. Analysis of the time series indicated an instantaneous pressure head > 0.5 m met the submergence criteria. Three cases of decreasing data quality illustrate these quality criteria choices (Figures 17, 19, and 21).

2. Coherence Criteria

The coherent Doppler is based upon pulse-to-pulse transmissions used to measure the along-beam component of current velocity (Stanton, 1996). Low phase coherence occurs primarily when signal levels at a given bin are very low, which is caused by

scattering attenuation in the earlier range bins. The quality of velocity, as well as returned backscatter in counts squared C^2 profiles, can be evaluated via the mean of the coherence for the lower half of range bins. Analysis of a time series of linear regressions between coherence and the sediment concentration mass indicated an inverse relationship. Low coherence returned near the bottom boundary layer indicates bubble saturation in the nearfield bins that severely attenuate the acoustic energy and obscure the bed (Figures 18, 20, and 22). Analysis of coherence time series, when compared with time series of the backscatter, indicates that a mean coherence > .7 corresponds to a high quality return for the bottom boundary layer.

The number of observations that satisfy the above pressure and coherence criteria is divided by the total number of observations in order to determine the overall data quality factor.

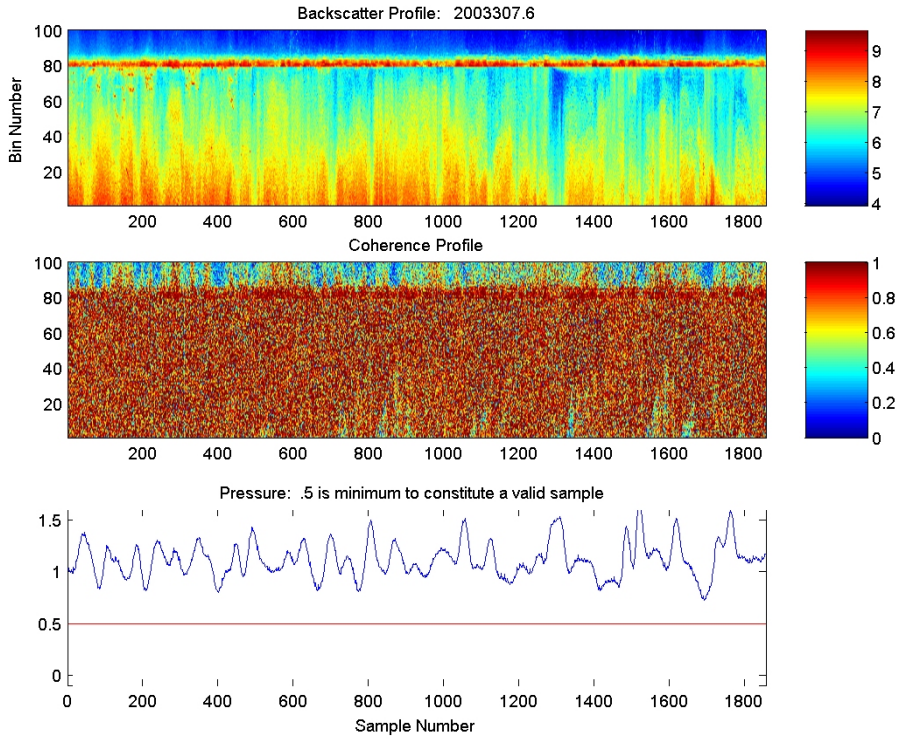

Figure 17. Backscatter, Coherence, and Pressure head. High Quality Data (100%). Notice that the pressure head is constantly above 0.5 m equivalent water height.

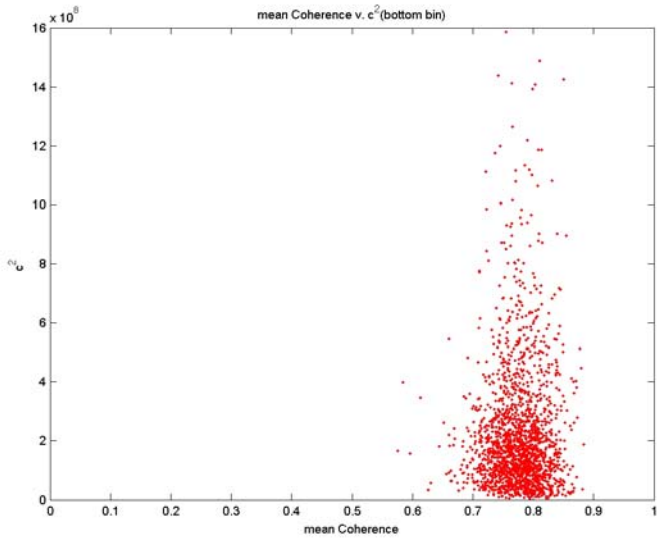

Figure 18. Mean Coherence v. Counts^2 from the same period as Figure 17. High Quality Data (100%). The mean coherence value is high, indicating a low level of attenuation.

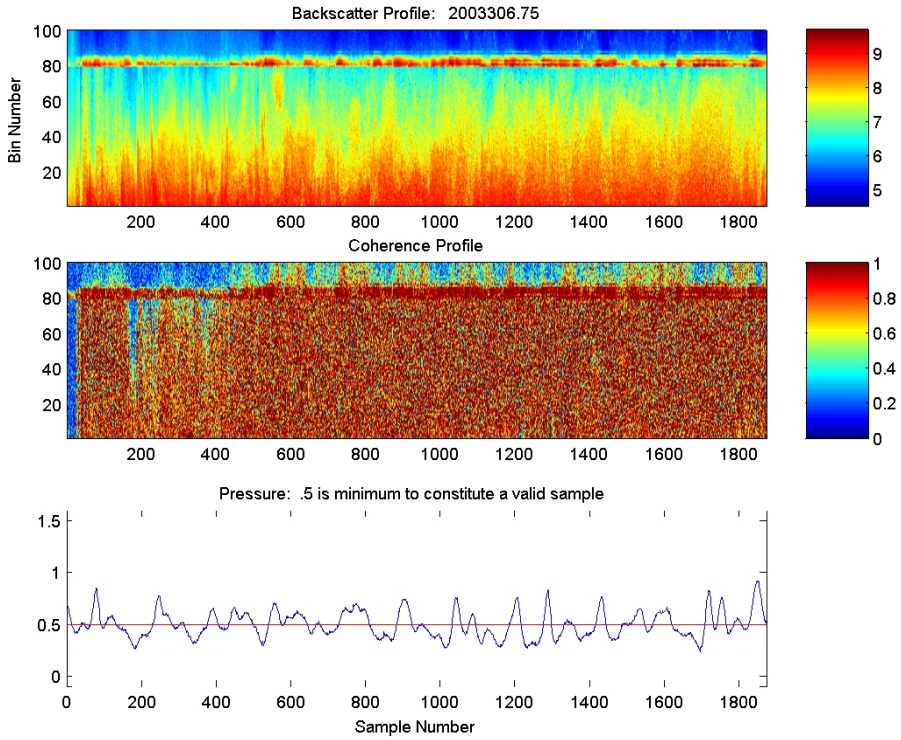

Figure 19. Backscatter, Coherence, and Pressure head. Medium Quality Data (46%). The pressure head indicates wave breaking over the BCDV. Notice the saturation of the upper bins (1-20) of returned backscatter profile.

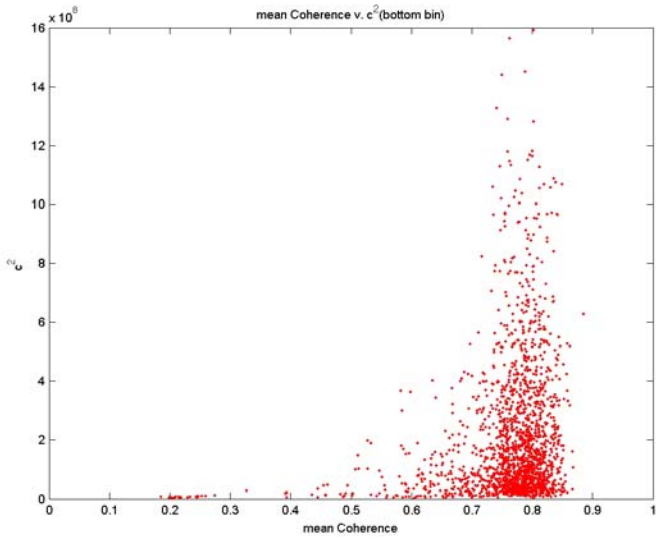

Figure 20. Mean Coherence v. Counts^2 from the same period as Figure 19. Medium Quality Data (46%). Coherence is negatively skewed, indicating attenuation in the nearfield. This corresponds to the saturation of the upper bins seen in the backscatter profile.

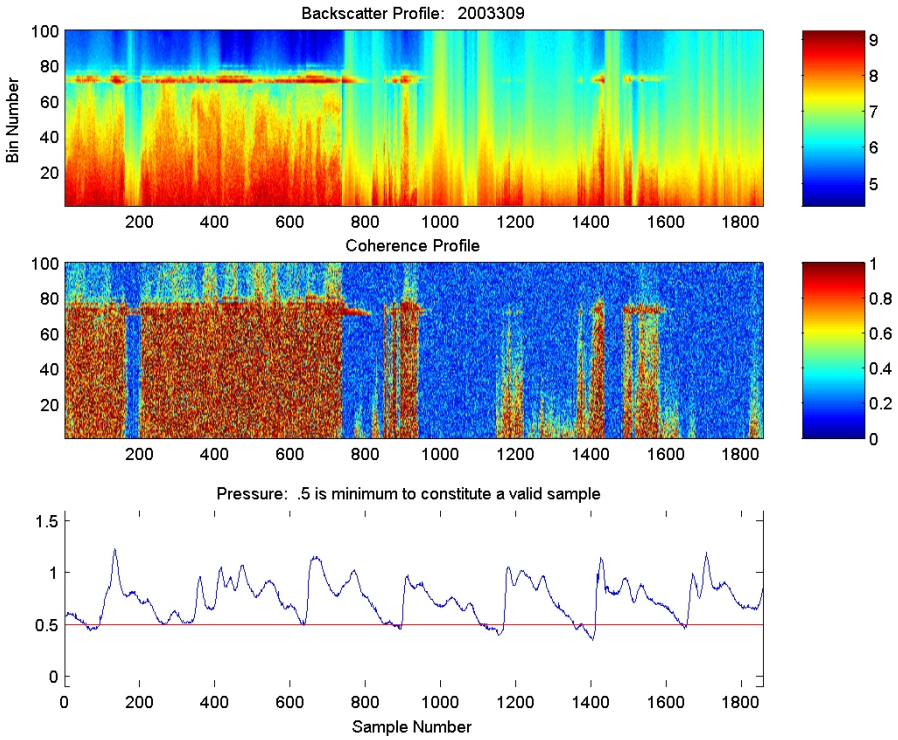

Figure 21. Backscatter, Coherence, and Pressure head. Low Quality Data (0%). The profiles indicate intense waves breaking near the transducer, entraining a dense concentration of air bubbles into the upper water column. Attenuation due to the presence of bubbles in the nearfield of the transducer can be seen to obscure the bed.

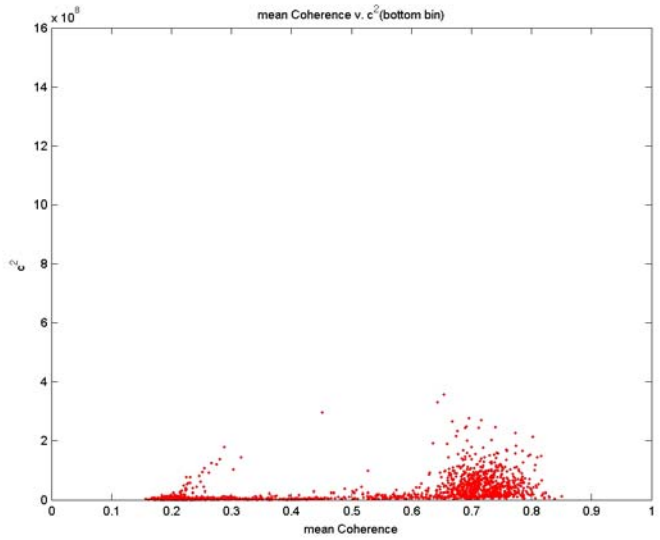

Figure 22. Mean Coherence v. Counts^2 from the same period as Figure 21. Low Quality Data (0%). A lack of coherence return indicates significant attenuation.

THIS PAGE INTENTIONALLY LEFT BLANK

III. RESULTS

A. OFFSHORE WAVE CONDITIONS DURING NCEX

Offshore significant wave heights observed from late October through early November were on average between .5 and 1 m and predominately shore normal. Yearday 304.5 exhibited the greatest wave heights, with a rapid build up from .5 to 1.4 meters over 24 hours propagating from 280 degrees (Figure 23). The other notable wave event occurred on yearday 307.5 with an increase from .8 to 1.1 m over a 24 hour period and propagating from 280 degrees (Figure 24). These incidents of increased offshore wave height are important to understanding the general energetics of the surf zone, as the breaking waves impart momentum flux to the water column which drives the nearshore current.

B. NEARSHORE INSTRUMENT ARRAY OBSERVATIONS

Instantaneous profiles of the sediment concentration and cross-shore/long-shore velocity were measured at the bottom boundary layer frame during periods of high tide over a consecutive sixteen day period in which significant sediment transport occurred resulting in local morphological changes.

Analysis of the offshore wave conditions, sediment flux velocity profiles, and corresponding morphology over a seven day subset of this time series shows the life cycle of a weak rip channel. The formation and infilling of the channel illustrates the relative importance of wave asymmetry and radiation stress driven currents in net sediment transport. An analysis of boundary layer structure, nearshore circulation, and morphology changes for this time series follows.

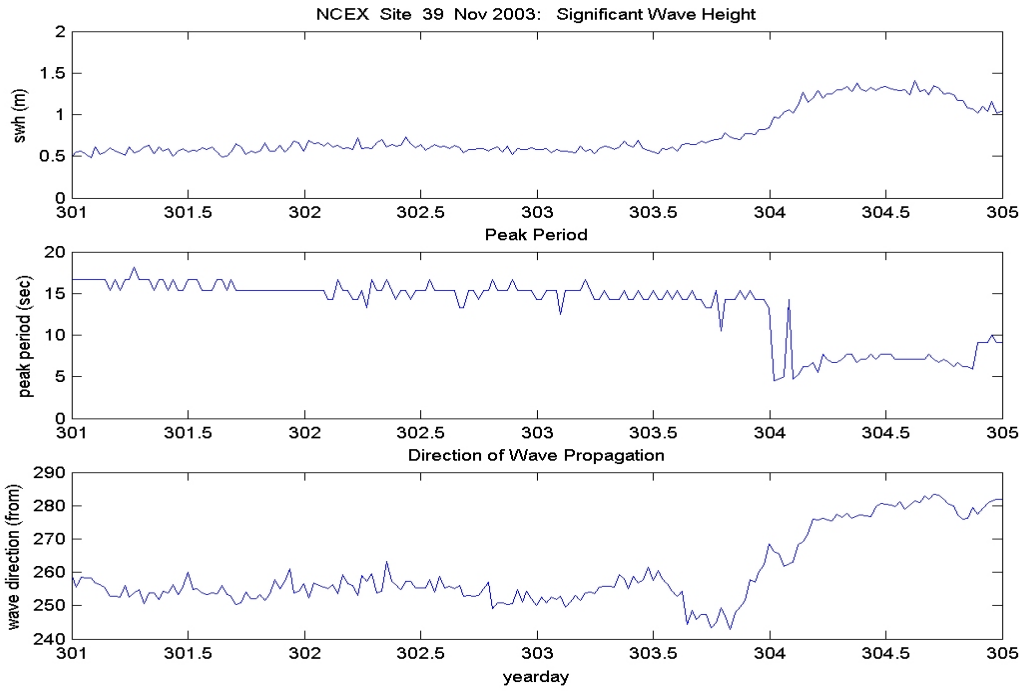

Figure 23. Offshore wave conditions for Black's Beach: 28 - 31 October 2003.

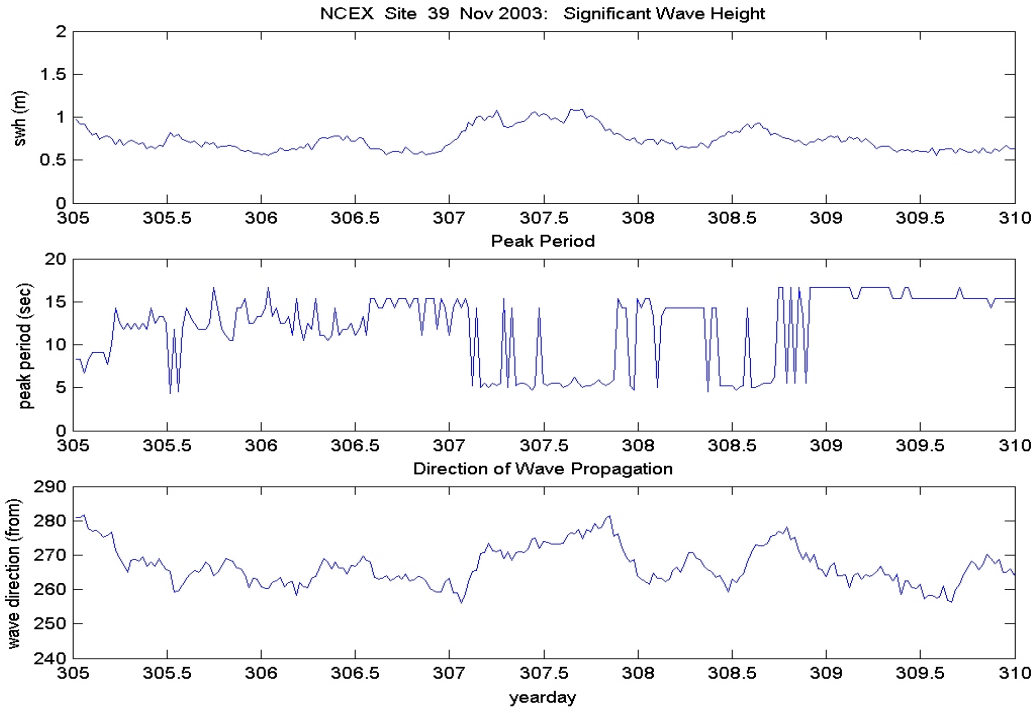

Figure 24. Offshore wave conditions for Black's Beach: 01 – 05 November 2003.

1. Yearday 303.639

Wave conditions were mild with an average height of 0.6 m (Figure 23). These low-energy conditions, coupled with the broad, flat nature of Black's Beach at the northern field site, resulted in a weak radiation stress driven cross-shore current in the offshore direction having a hourly mean magnitude of 0.07 ms^{-1} (Figure 25). A consistent offshore direction is seen in all cross-shore currents profiles on two minute averaging scales with the magnitude of the velocity varying. Profiles of cross-shore velocity skewness and kurtosis reveal onshore asymmetries in the wave induced momentum, indicating the presence of non-linear onshore bores within the surf zone. These asymmetries are generated when the wave's orbital cycle is disturbed during shoaling and, in lack of significant offshore flow from the cross-shore current, will cause accretion of the sediment onshore.

Profiles of the net sediment flux show the presence of a thin bottom boundary layer dominated by wave induced velocities within 2 to 4 cm of the bed (Figure 25). This bottom boundary layer is present in all measured profiles and demonstrates the importance of wave induced momentum flux to the sediment transport process. Analysis of the net sediment flux profile from yearday 303 shows an onshore flux of 0.4 $gl^{-1}ms^{-1}$, indicating that wave asymmetry dominants over the weak offshore mean current in sediment transport in these low energy conditions. This is directly supported by Figure 26, an Argus pixel variance image of waves breaking over the morphology within the surf zone, which shows a well defined bar system with few longshore breaks, indicative of prolonged onshore sediment transport. The BCDV is situated approximately 11 m shoreward from the offshore edge of the bar.

2. Yearday 305.929

During the next two days, yearday 304 and 305, offshore wave conditions increased from 0.6 to 1.4 m in a period of 12 hours (Figure 23). As the H-frame was set too high, BCDV data to the bed is unavailable for the majority of this period, although successful measurements were obtained during the later high tide on yearday 305 (305.9292), coinciding with the conclusion of elevated wave heights (Figure 24). The

following observations illustrate the affects of the increased momentum flux imparted by the radiation stress of energetic waves.

The measurements of the hourly mean nearshore currents, returned by the PUV sensor array, indicate flow in an onshore direction near the BCDV H-frame, and a higher magnitude offshore flow to the south (Figure 28). The onshore flow near the H-frame is a result of the increased wave asymmetry and is recorded in the in bottom boundary layer cross-shore current profiles measured by the BCDV (Figure 27). The hourly mean cross-shore current, at 0.2 m above the bed is offshore with 0.06 ms^{-1} magnitude and 0.02 ms^{-1} 1 cm above the bed. This is in contrast, however, to the resultant skewness of cross-shore velocity that is at its maximum magnitude for the experiment, representing the strongest recorded onshore momentum due to wave asymmetry. The predominate onshore momentum has produced a net sediment flux that is doubled in magnitude (0.8 $gl^{-1}ms^{-1}$) from the previous profile and results in an elevation gain of 0.1 m in the bed height as measured by the BCDV over a 48 hour period (not shown).

Although bores associated with the energetic wave activity have caused bar accretion at the survey site, the increased return flow, seen in the offshore tending current measurements south of the instrument frame, has resulted in the formation of a weak rip channel. This channel, indicated on the variance image as a dark area in between the lighter (shallower) sand bars and creates a cross-shore break in the bar south the instrument frame (Figure 29).

3. Yearday 306.554

Offshore wave conditions have reduced to 0.5 m (Figure 24). Mean nearshore currents have turned to a uniformly offshore direction at the location of the cross-shore PUV array (Figure 31). The net cross-shore velocity in the bottom boundary level has rapidly increased to over double the magnitude of the previous profile while the cross-shore current 5 cm above the bed has dramatically increased from 0.05 m/s to 0.12 m/s, reflecting significant offshore flow (Figure 30). Cross-shore velocity skewness and kurtosis profiles indicate no change in the wave asymmetry suggesting no change in this

onshore driver. This is certified by the net sediment flux that has shifted to the offshore direction at a magnitude of 0.3 $gl^{-1}ms^{-1}$.

The rip channel break is also seen on the brightness variance image, showing that the instrument frame is now within the dark return area associated with the deeper water of the rip channel (Figure 32). The placement of the BCDV within the center of the rip channel allowed the influence of cross-shore current and morphological bar evolution on sediment transport to be uniquely demonstrated.

4. Yearday 307.0192

Conditions observed by the BCDV between yearday 306.5542 and 307.0192 remain the same, with the exception of wave asymmetry. The PUV sensor array measured mean nearshore currents with an offshore direction aligned with the break in the bar system and with a small southern longshore current aligned with the skewed rip channel (Figure 34). Cross-shore velocity skewness and kurtosis profiles reveal diminishing onshore skewness, as compared with previous profiles, indicated by the wave profiles becoming more linear (Figure 33). The rip channel spanning the H-frame now appears to be connected to a small feeder trough just to the North of the cross-shoe array (Figure 35).

5. Yearday 307.5542

Offshore wave conditions show an increase in wave height to 1.1 m (Figure 24). The cross-shore current profile indicates a slight decrease in the velocity magnitude within the wave boundary layer, while the wave asymmetries display elevated magnitudes near the bed (Figure 36). The cross-shore sediment flux profile shows a slight offshore flux of 0.1 $gl^{-1}ms^{-1}$, indicating a near balance between wave asymmetry and cross-shore current components of sediment transport.

Although lower in magnitude, the predominant influence of cross-shore current acting in association with topography is demonstrated by the growth of an offshore bulging in the bar, and a broadening of the high variance breaking area due to the

stronger wave forcing. Offshore sediment transport has caused the bar to extend 24 m offshore (Figure 38).

6. Yearday 308.0592

Offshore waves heights decrease to 0.8 m (Figure 24). The mean nearshore current measured by the cross-shore PUV array shows flow in an offshore direction, illustrating the continued presence of the rip channel (Figure 40). A decrease in the magnitude of the cross-shore current velocity in the wave boundary layer, when compared with previous measurements, as well as a decrease in the net offshore flux to 0.1 $gl^{-1}ms^{-1}$ indicates that the rip channel is state of transition (Figure 39). This weak offshore flux is sufficient, however, to ensure continued growth of the offshore bulge, shown on the brightness variance image as a bright area extending offshore approximately 70 m north of the H-frame (Figure 41).

7. Yearday 309.0792

The skewness and kurtosis profiles display a significant increase in magnitude within the wave boundary layer, indicating the return of narrow, high amplitude onshore momentum fluxes associated with the presence of bores (Figure 42). The onshore wave forcing is offset by a weak offshore velocity, and the resultant net sediment flux is almost zero, with a slight onshore peak to 0.3 $gl^{-1}ms^{-1}$ at 1 cm above the bed. The lack of a unified offshore direction in the hourly mean current (Figure 43) and the end of offshore sediment flux indicates the completion of the cycle of morphological evolution associated with the rip channel, as evidenced by the lack of change in the bar between Figure 41 and Figure 44. A significant increase in bed height measurements is recorded by the BCDV between yearday 307 and 309. The bed height under the instrument frame doubled from 0.3 m to 0.6 m in a 48 hour period as the rip channel began to fill, forcing the elevation of the BCDV (seen as a decrease in distance of the bed return to the transducer face in Figure 45 and Figure 46), indicating that wave asymmetry has returned as the predominate sediment transport mechanism.

THIS PAGE INTENTIONALLY LEFT BLANK

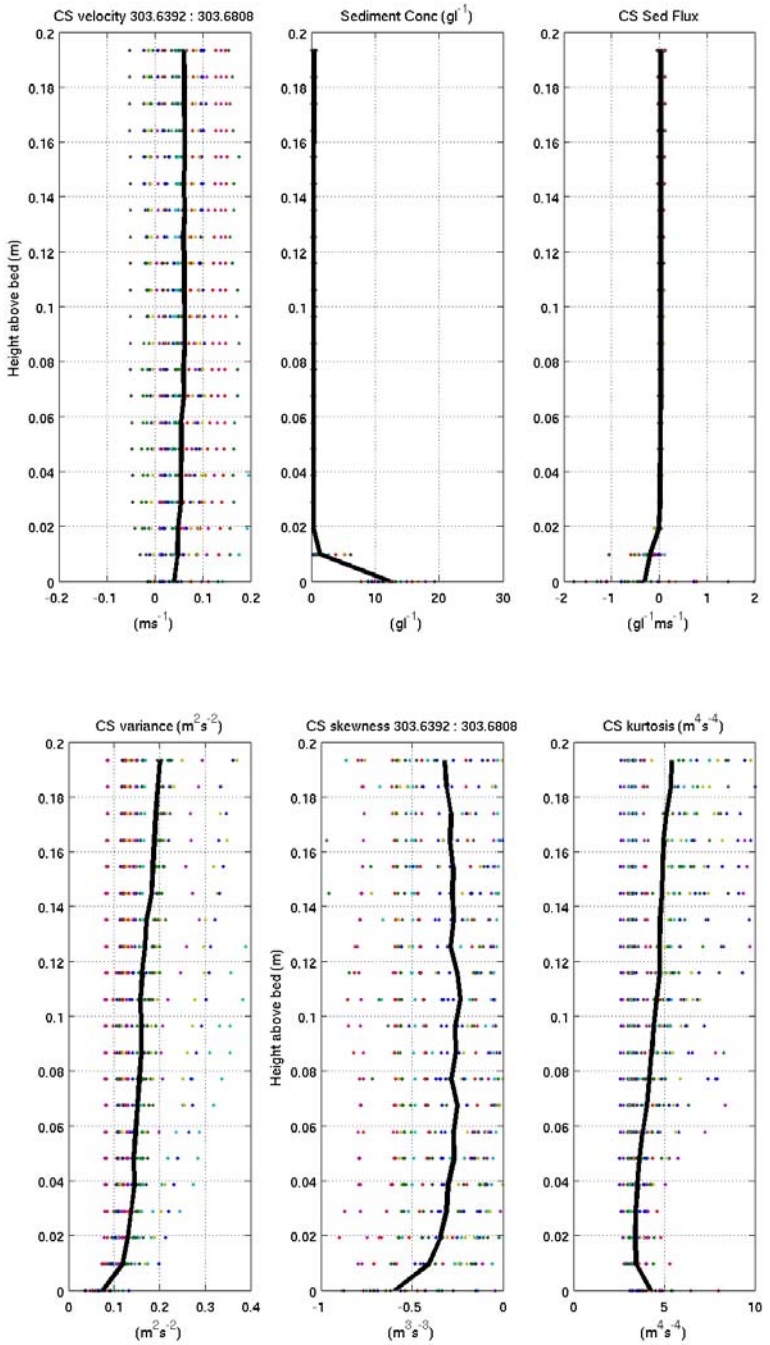

Figure 25. Profiles of Cross-Shore Velocity, Sediment Concentration, Sediment Flux, Variance, Skewness, and Kurtosis for yearday 303.6392.

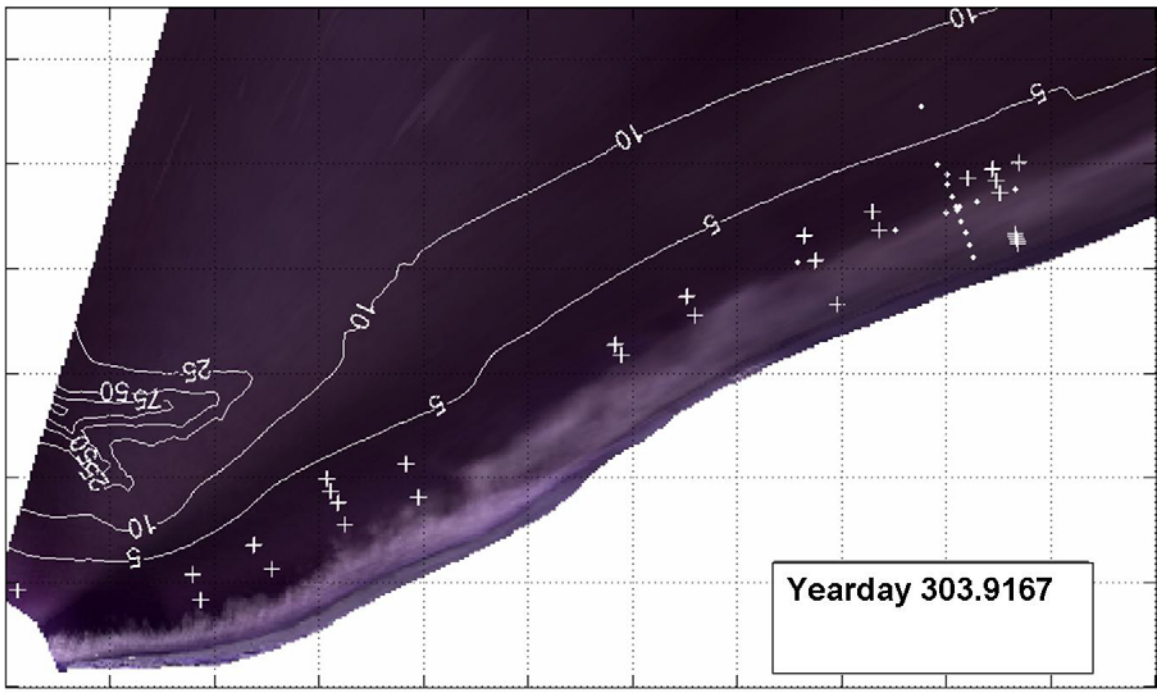

Figure 26. Variance image of NCEX surf zone during mid-day: 303.9167. Courtesy of the Coastal Imaging Laboratory, Oregon State University.

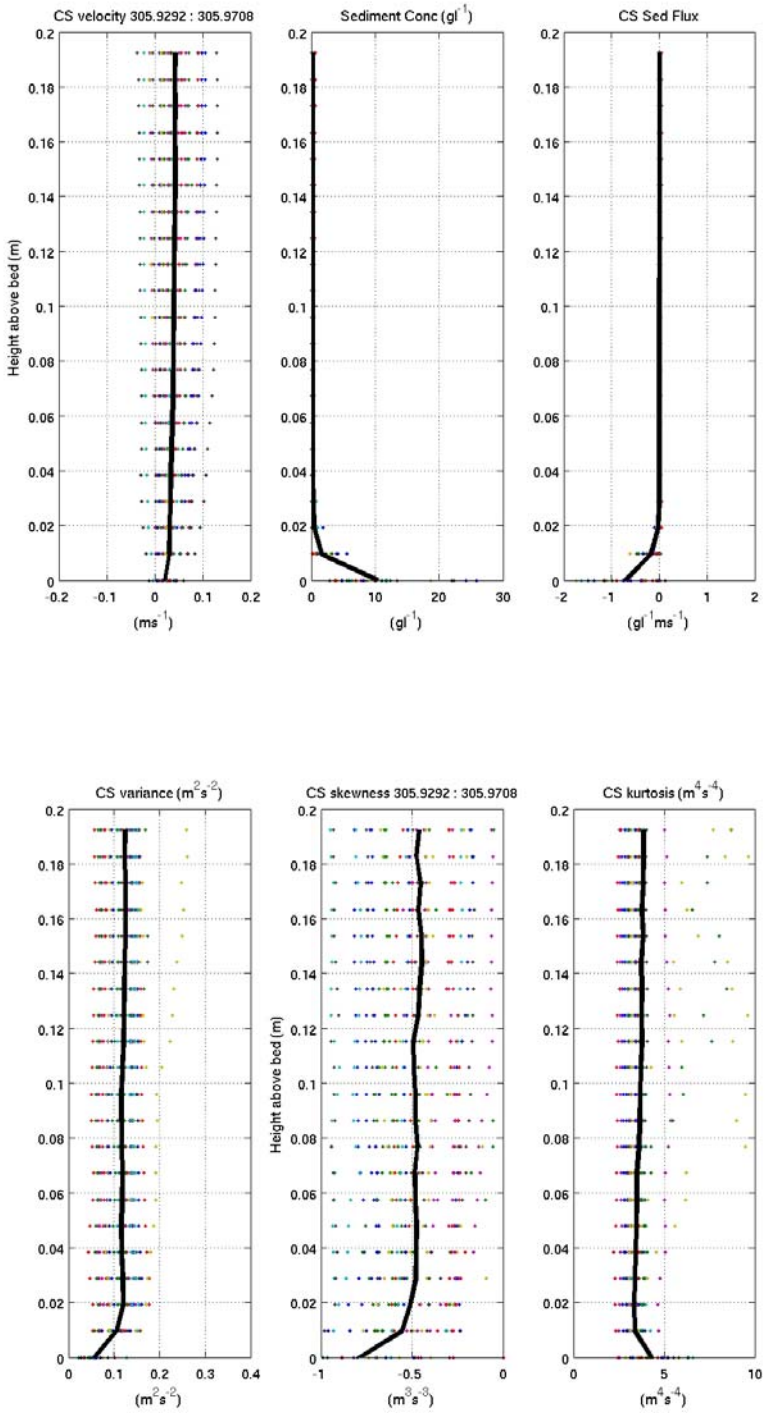

Figure 27. Profiles of Cross-Shore Velocity, Sediment Concentration, Sediment Flux, Variance, Skewness, and Kurtosis for yearday 305.9292.

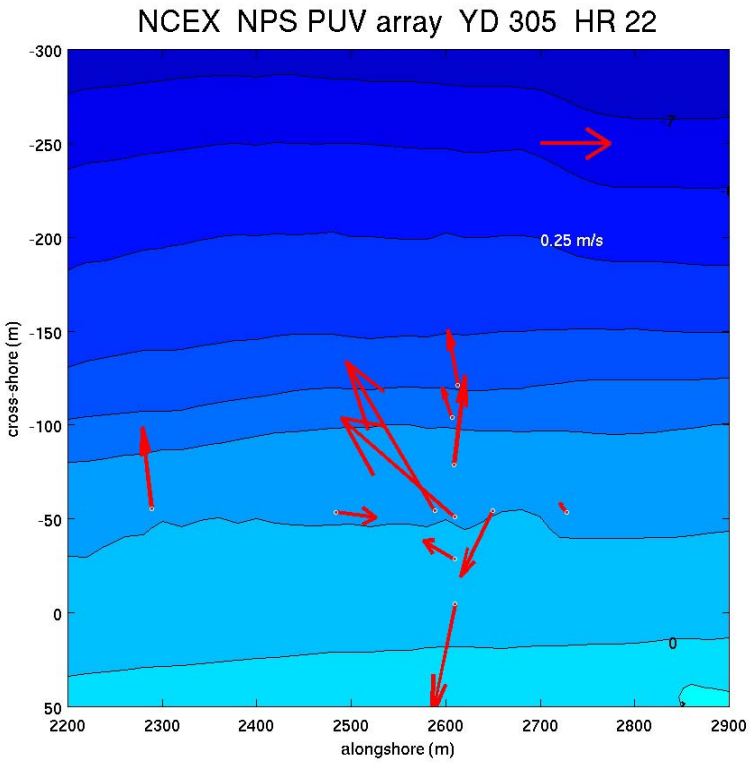

Figure 28. Mean Nearshore Current Observation associated with yearday 305.9292.

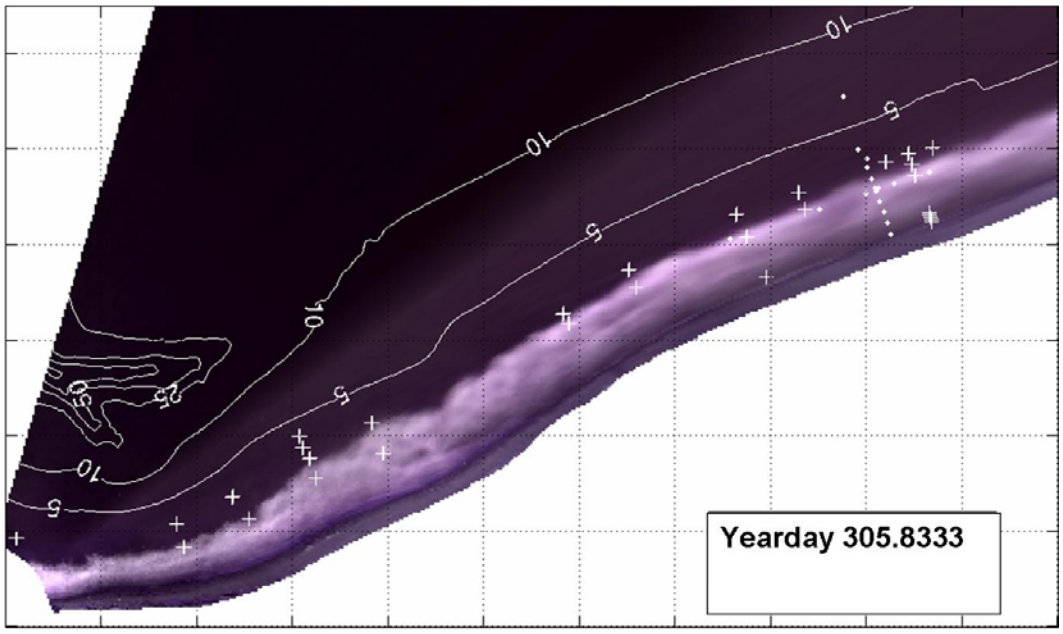

Figure 29. Variance image of NCEX surf zone during mid-day: 305.8333. Courtesy of the Coastal Imaging Laboratory, Oregon State University.

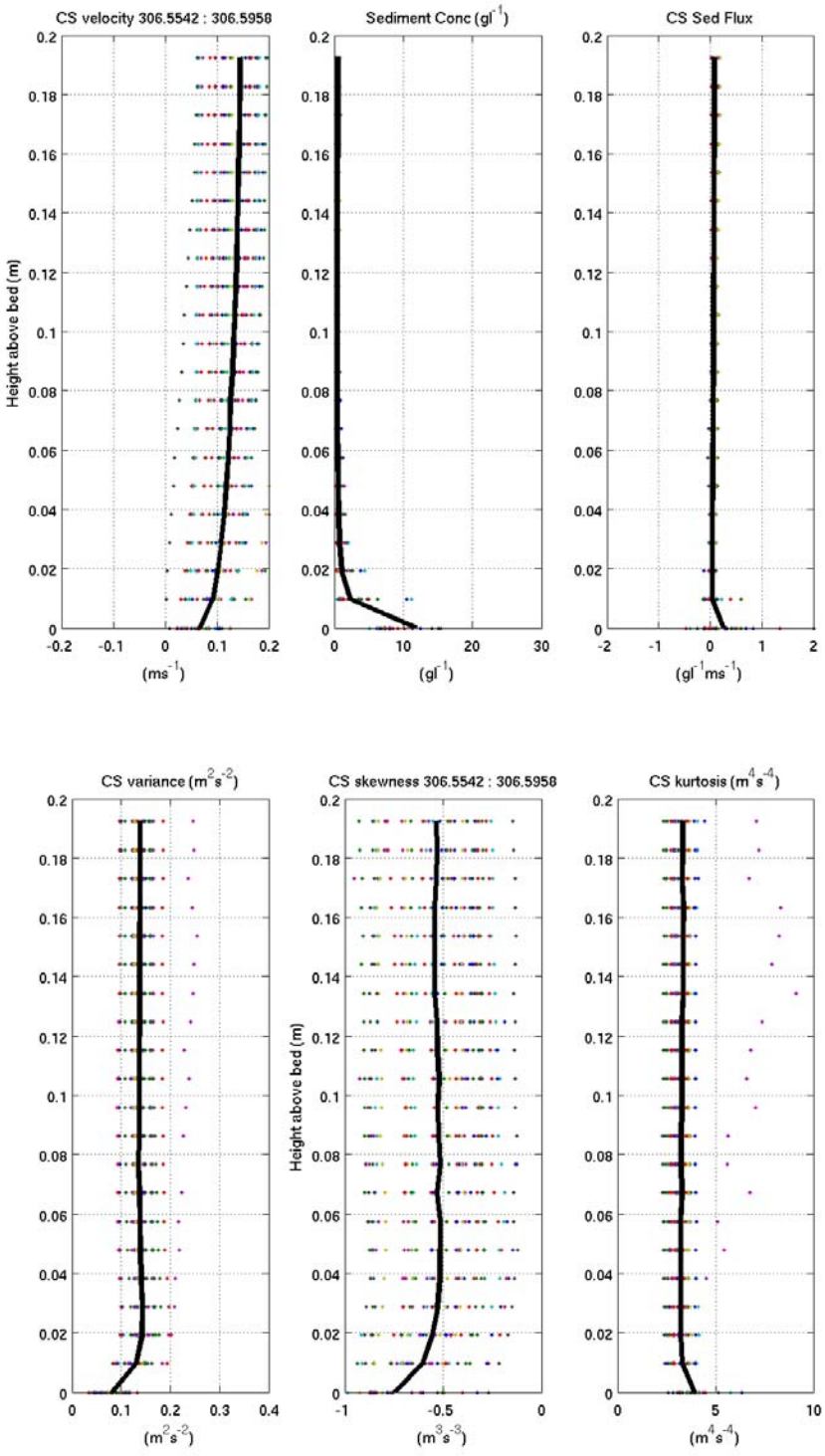

Figure 30. Profiles of Cross-Shore Velocity, Sediment Concentration, Sediment Flux, Variance, Skewness, and Kurtosis for yearday 306.5542.

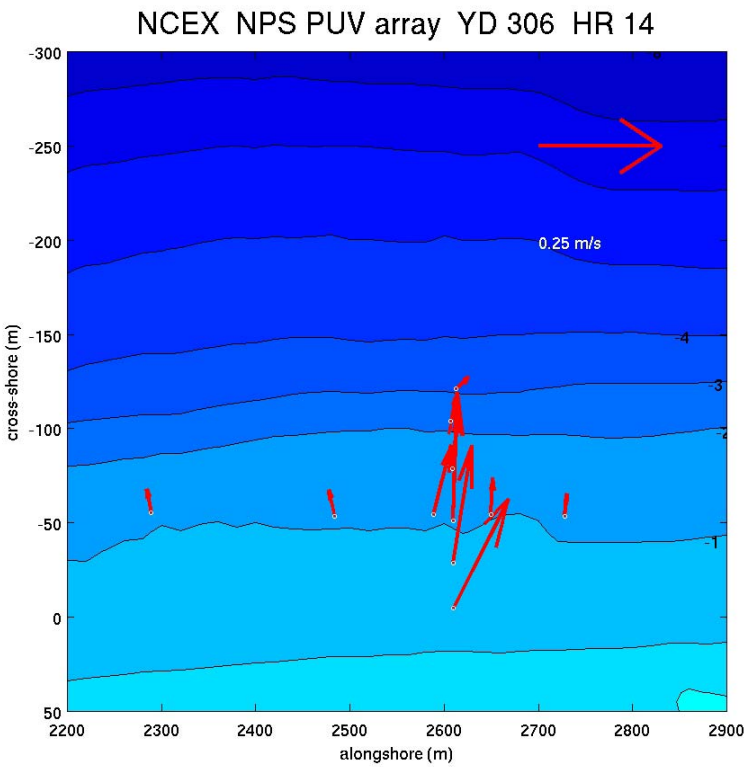

Figure 31. Mean Nearshore Current Observation associated with yearday 306.5542.

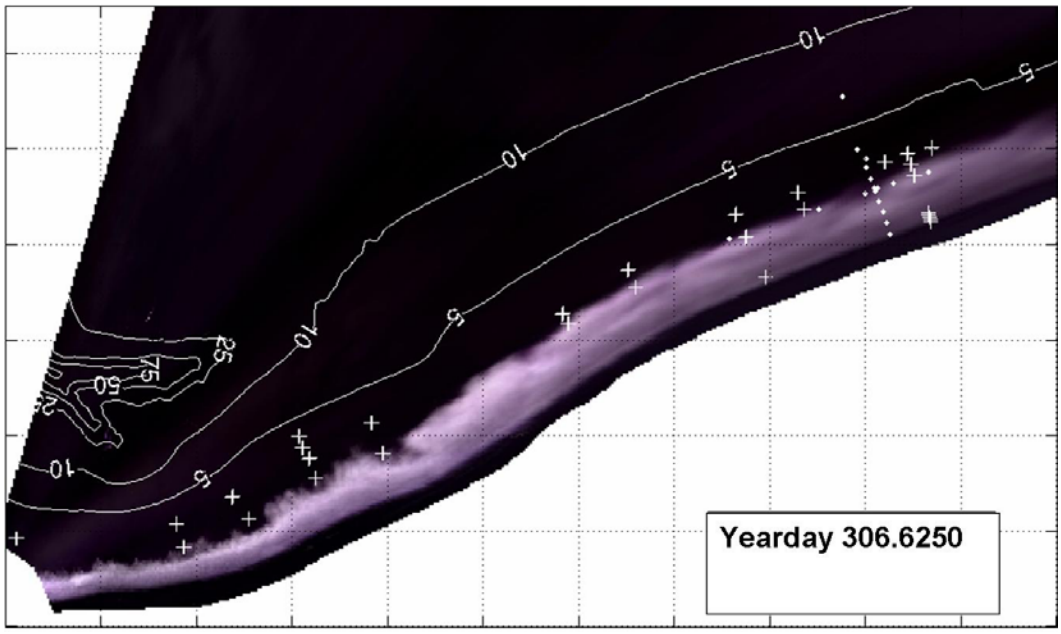

Figure 32. Variance image of NCEX surf zone during mid-day: 306.6250. Courtesy of the Coastal Imaging Laboratory, Oregon State University.

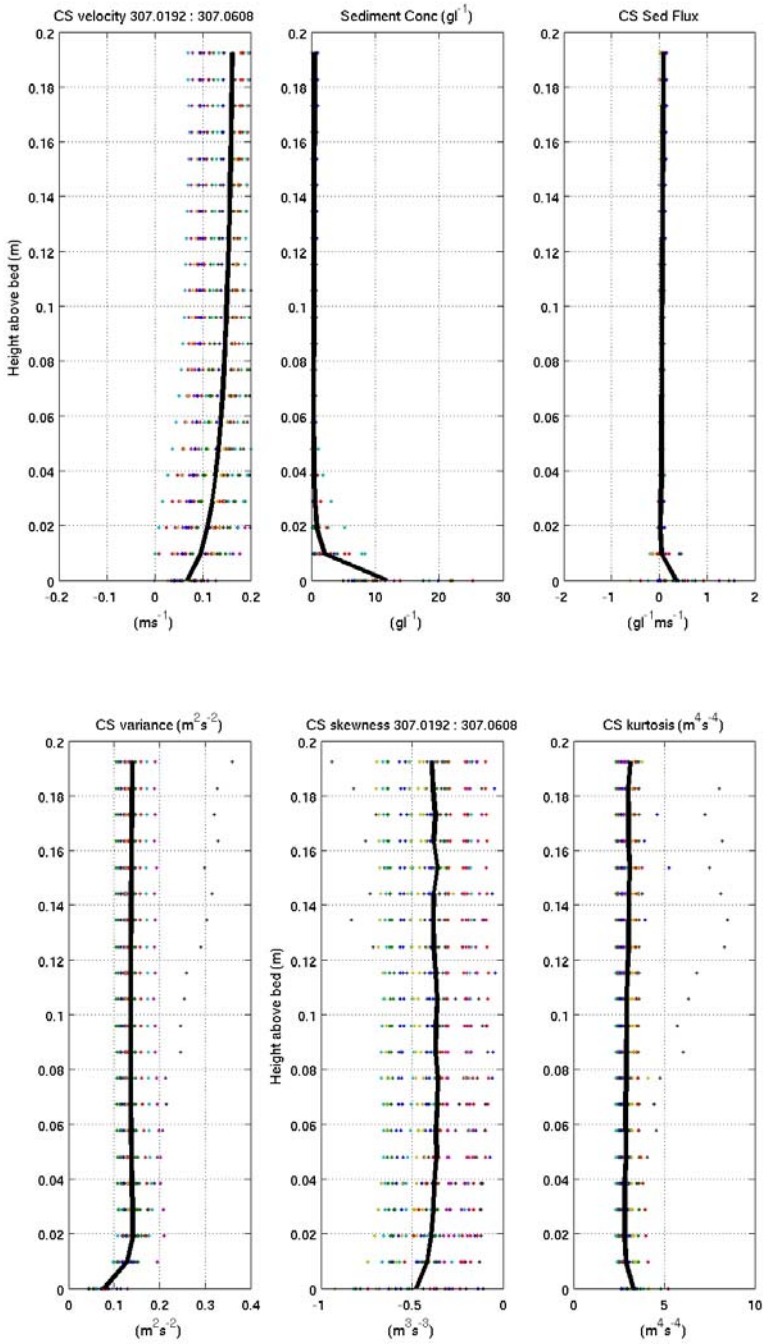

Figure 33. Profiles of Cross-Shore Velocity, Sediment Concentration, Sediment Flux, Variance, Skewness, and Kurtosis for yearday 307.0192.

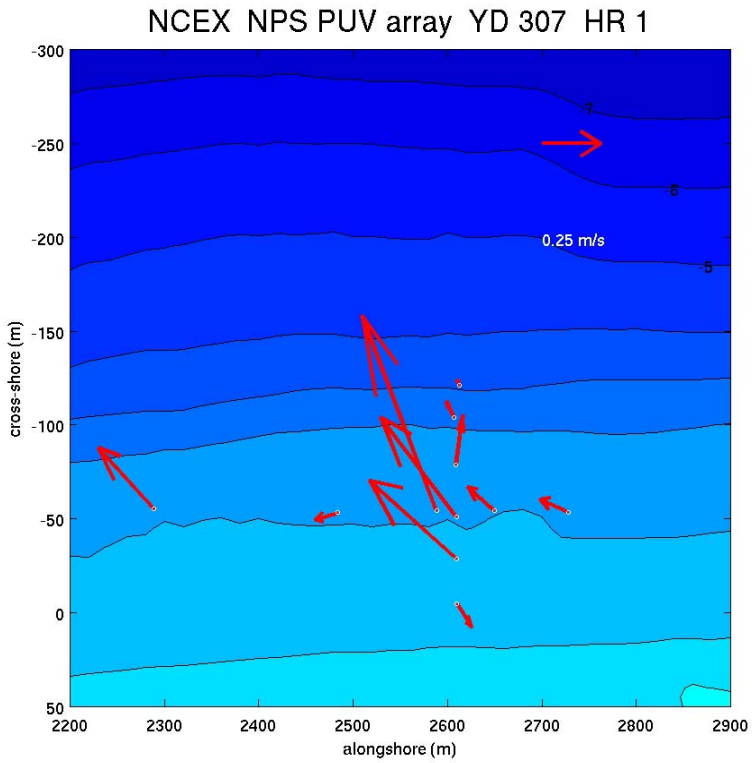

Figure 34. Mean Nearshore Current Observation associated with yearday 307.0192.

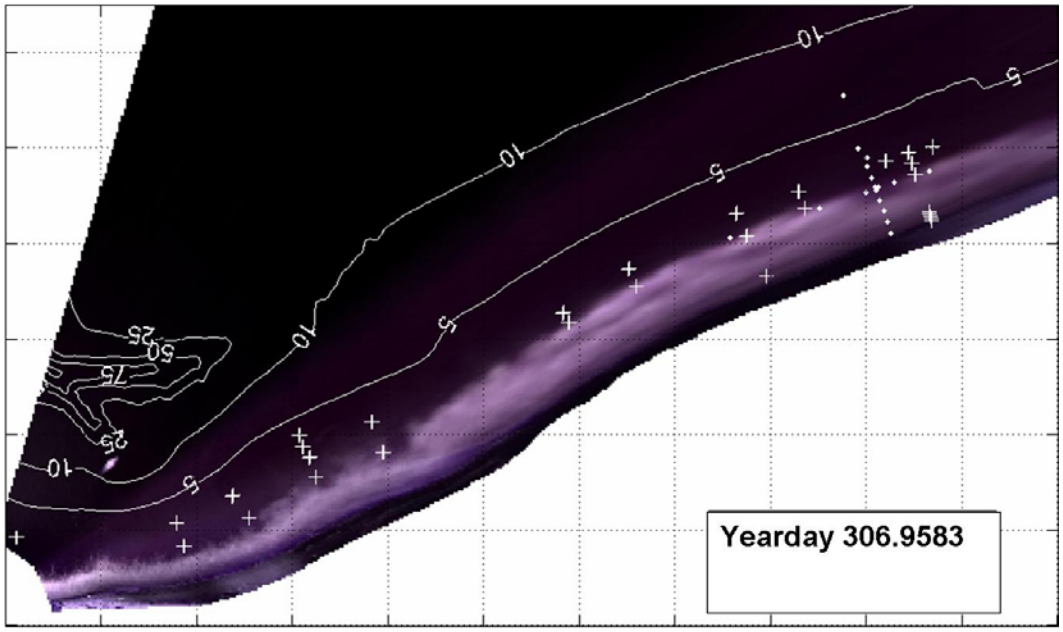

Figure 35. Variance image of NCEX surf zone: 306.9583 (closest available image to be paired with 307.0192). Courtesy of the Coastal Imaging Laboratory, Oregon State University.

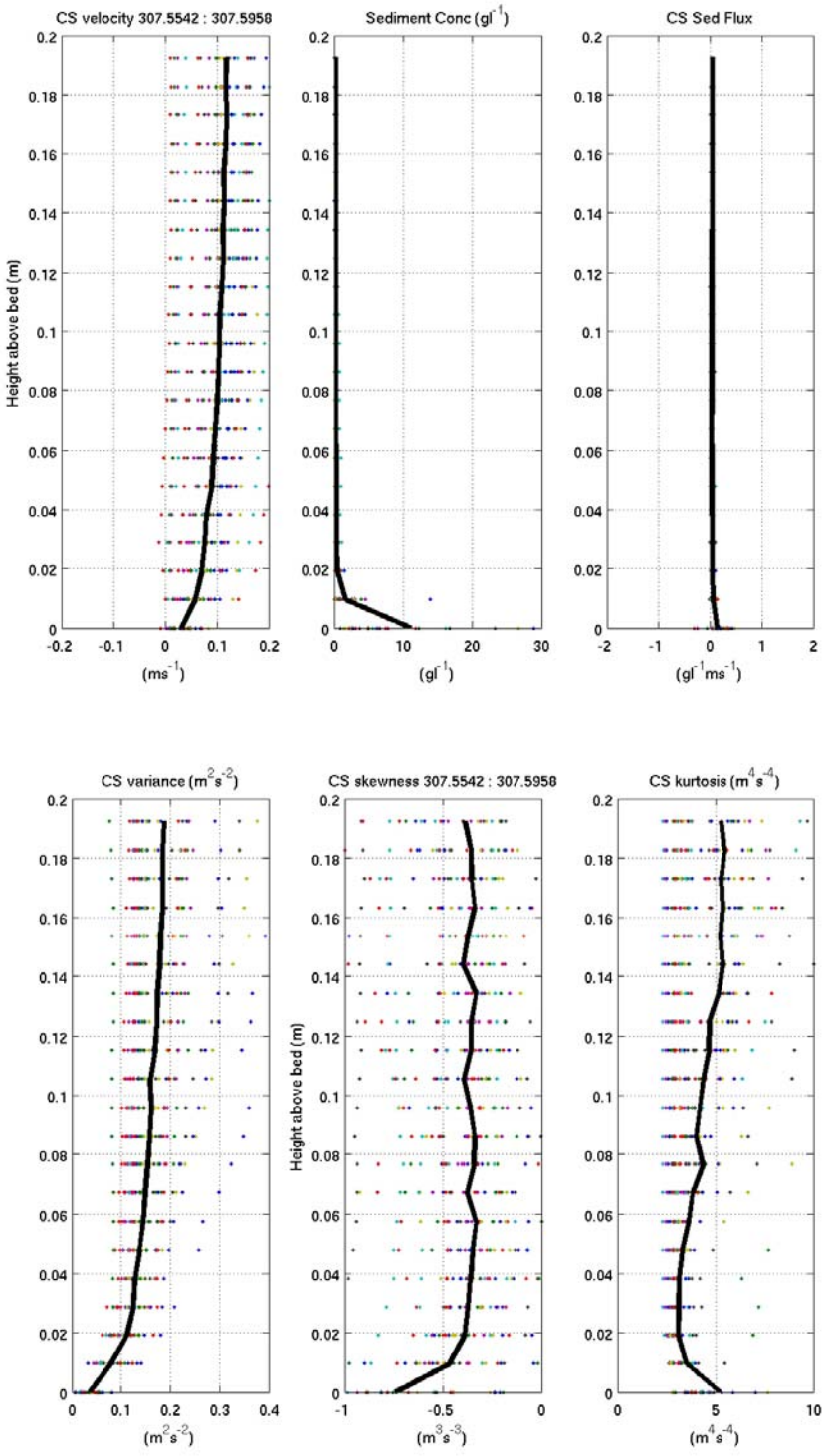

Figure 36. Profiles of Cross-Shore Velocity, Sediment Concentration, Sediment Flux, Variance, Skewness, and Kurtosis for yearday 307.5542.

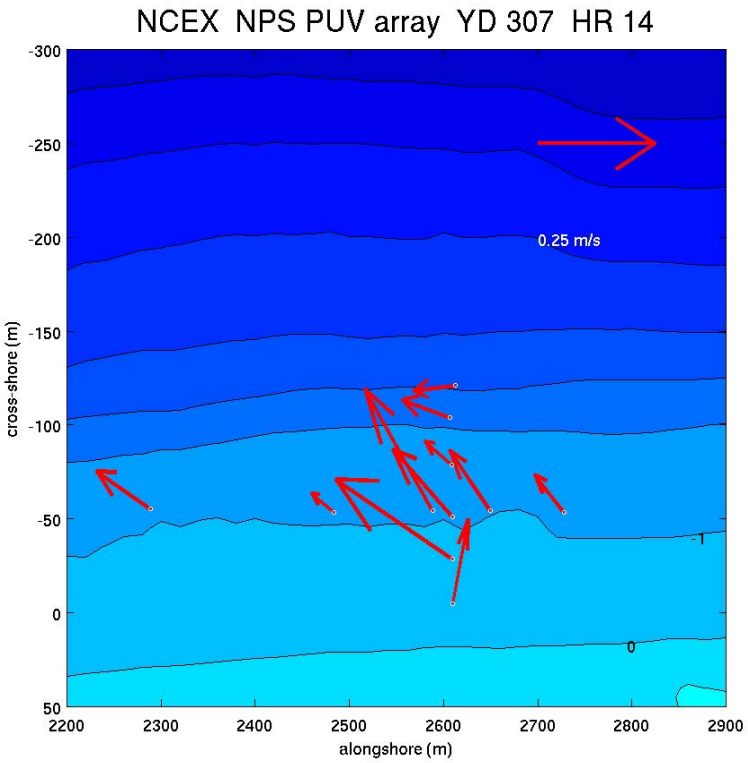

Figure 37. Mean Nearshore Current Observation associated with yearday 307.5542.

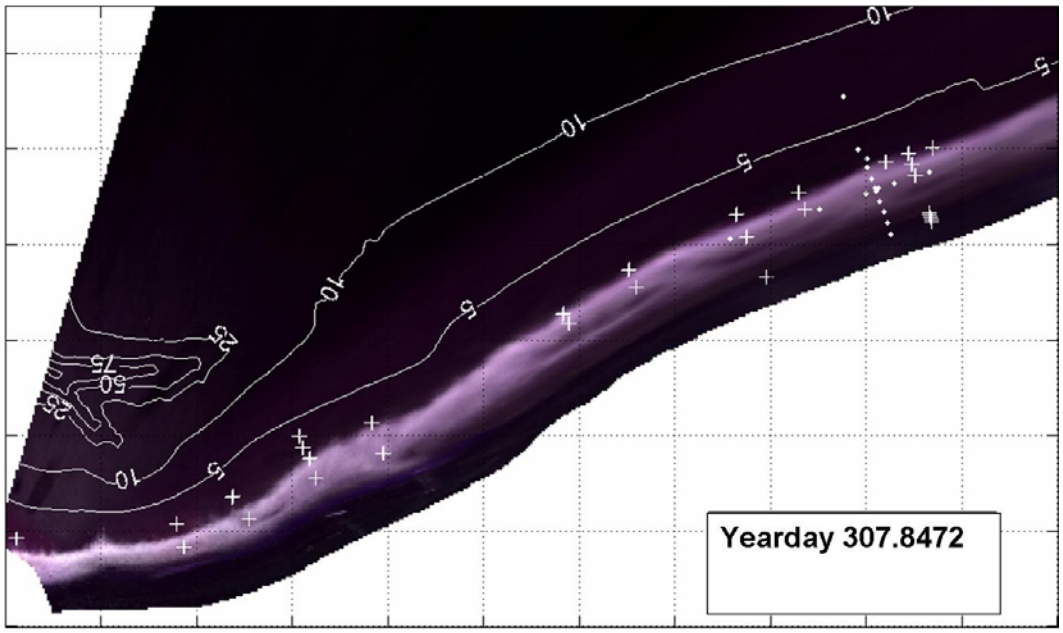

Figure 38. Variance image of NCEX surf zone during mid-day: 307.8472. Courtesy of the Coastal Imaging Laboratory, Oregon State University.

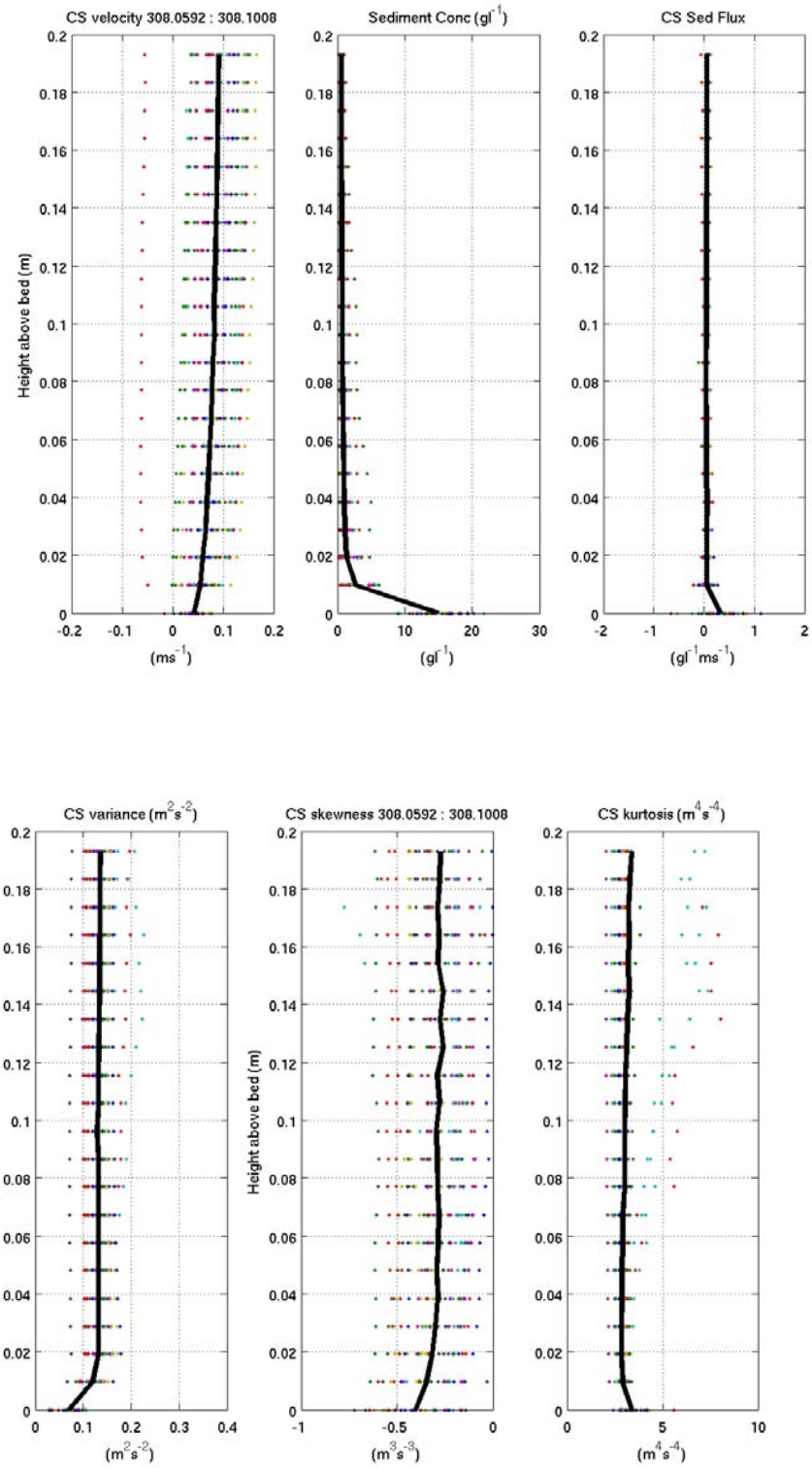

Figure 39. Profiles of Cross-Shore Velocity, Sediment Concentration, Sediment Flux, Variance, Skewness, and Kurtosis for yearday 308.0592.

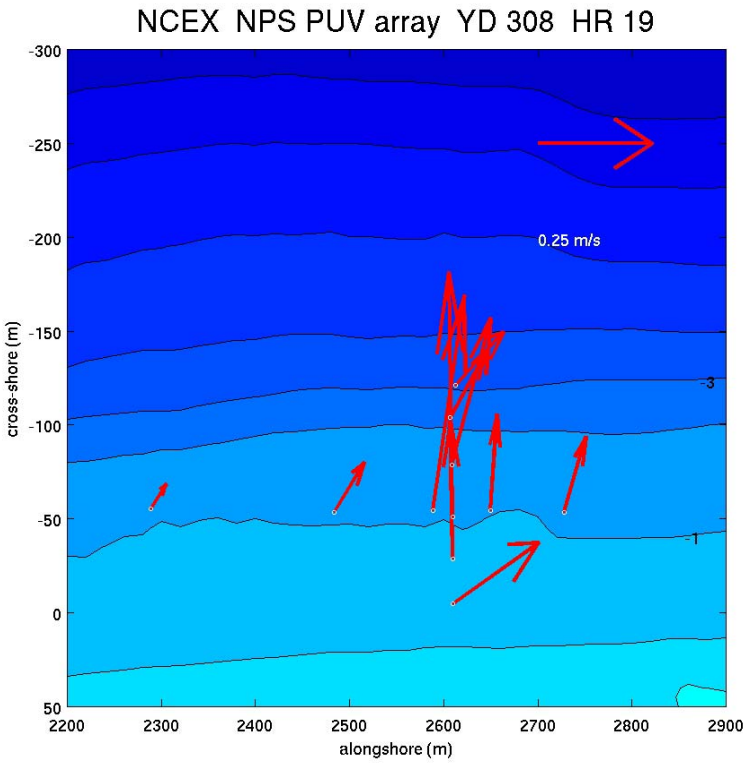

Figure 40. Mean Nearshore Current Observation associated with yearday 308.0592.

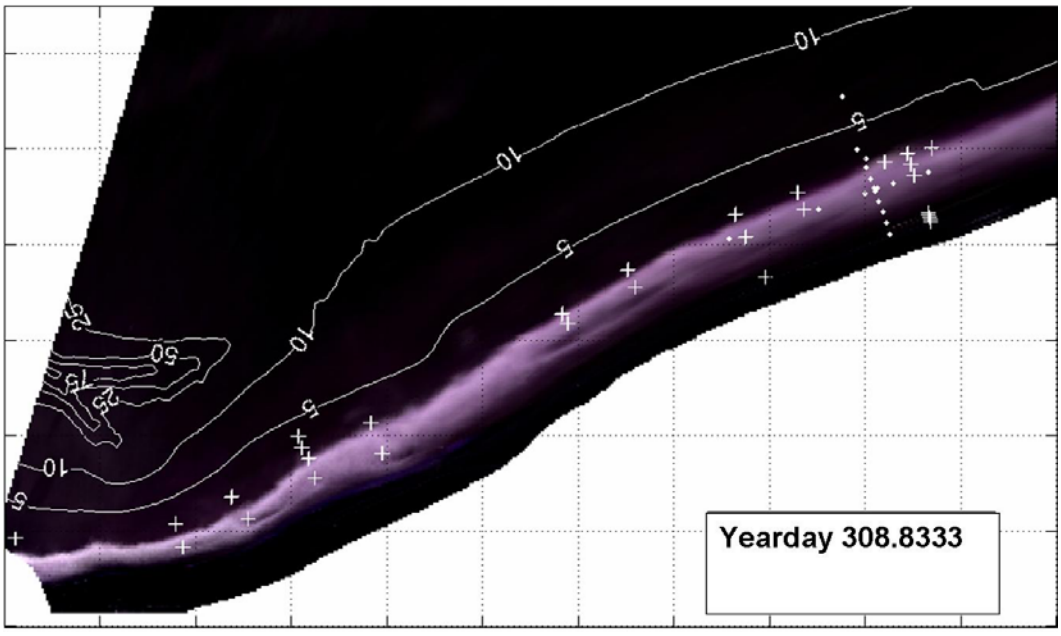

Figure 41. Variance image of NCEX surf zone during mid-day: 308.8333. Courtesy of the Coastal Imaging Laboratory, Oregon State University.

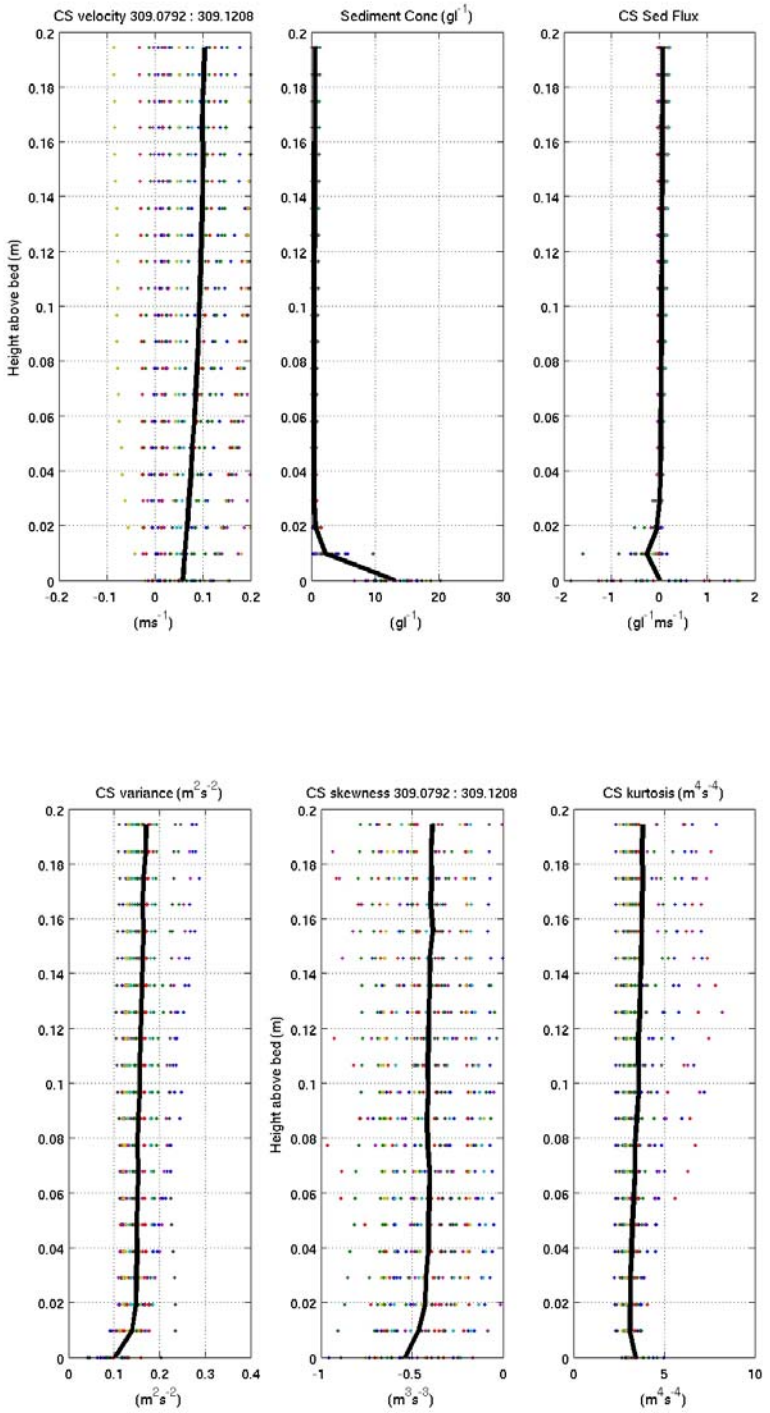

Figure 42. Profiles of Cross-Shore Velocity, Sediment Concentration, Sediment Flux, Variance, Skewness, and Kurtosis for yearday 309.0792.

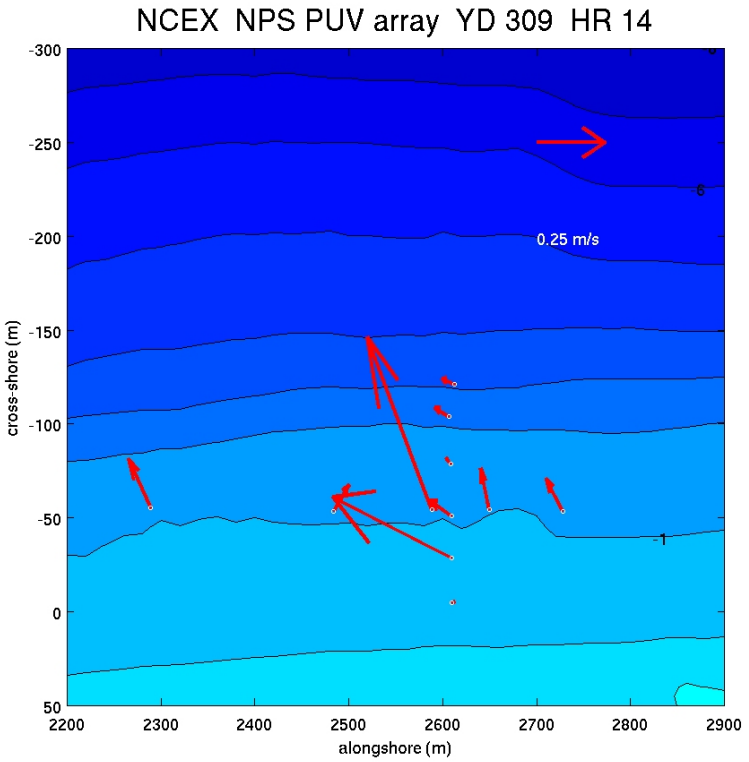

Figure 43. Mean Nearshore Current Observation associated with yearday 307.5542.

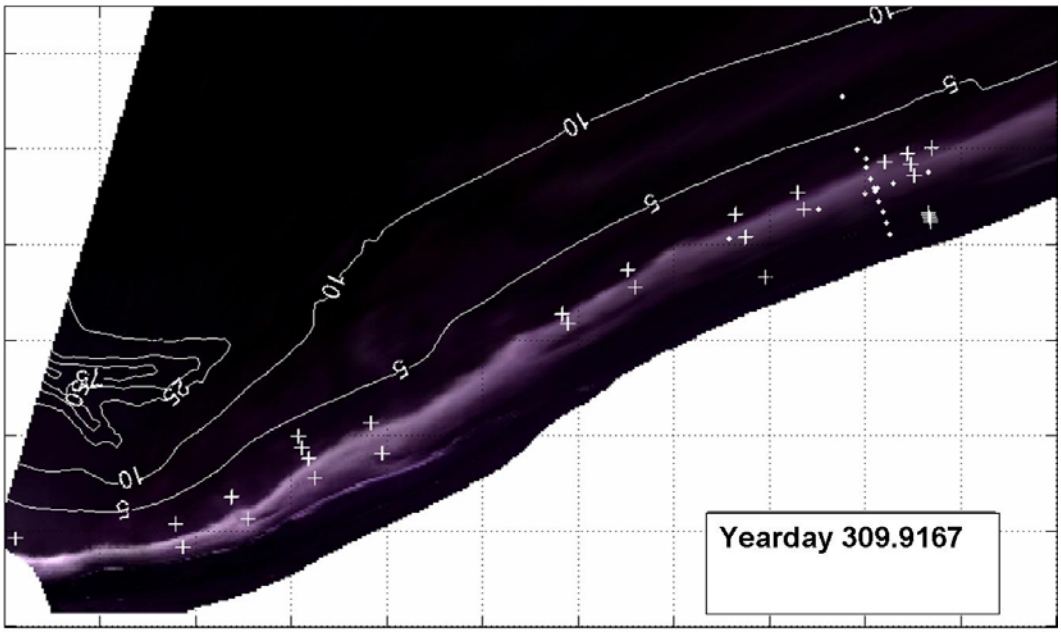

Figure 44. Variance image of NCEX surf zone during high tide: 309.9167. Courtesy of the Coastal Imaging Laboratory, Oregon State University.

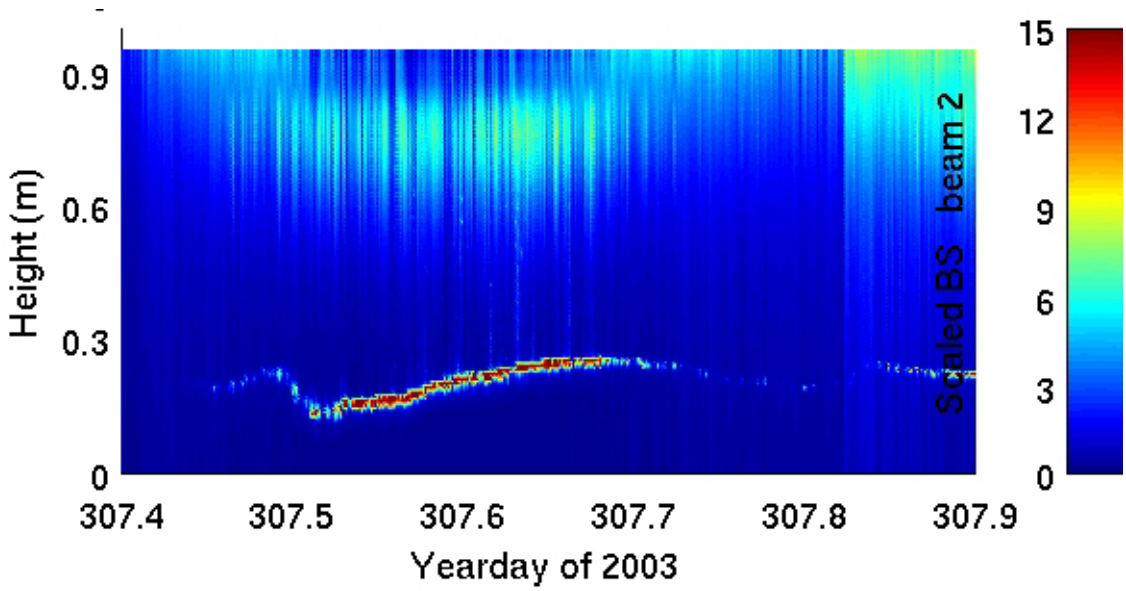

Figure 45. Time series of acoustic pressure returned by the BCDV showing the bed height (red) for yearday 307.

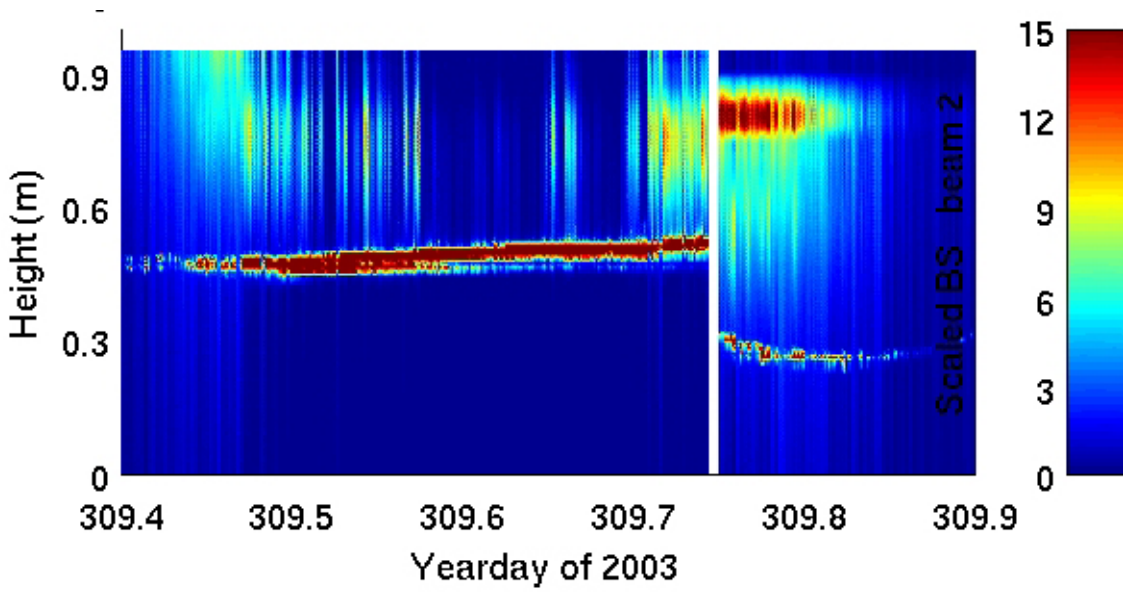

Figure 46. Time series of acoustic pressure returned by the BCDV showing the bed height (red) for yearday 309. The bed height doubles between yearday 307 and 309. The break in the time series (white line) shows were the BCDV was elevated. The increase in bed height signifies the completion of the rip channel and associated offshore sediment flux on yearday 308.

IV. DISCUSSION AND CONCLUSIONS

A. CONCLUSIONS

This thesis examined the use of high frequency acoustic backscatter as a means of directly measuring sediment concentration and flux profiles in the surf zone with the ultimate goal of comparing the resultant current velocity and sediment concentration profiles with existing models.

Scattering attenuation in the nearfield caused by bubbles entrained into the upper water column by breaking waves as well as the transducer coming out of the water during low tide or large waves are two potential sources of error that exist in using acoustic backscatter inversion to measure sediment flux in the surf zone. The use of pressure and coherence returns as criteria by which to evaluate data quality can limit these potential errors by excluding sample intervals contaminated by these effects. Acoustic backscatter inversion techniques, when calibrated with *in situ* sediment samples from the field site, provide high spatial and temporal resolution estimates of sediment concentration and resulting fluxes, even in the thin wave boundary layer associated with the flat, sandy bottom bar where the BCDV was mounted. These estimates of sediment flux qualitatively correlate with observed mean currents and the evolution of a rip channel, showing a strong morphological response to the sediment flux.

Cross-shore velocity profiles, when compared with the profiled cross-shore wave forcing characteristics and resultant sediment flux, demonstrated that three-dimensional radiation stress forced currents, acting in conjunction with a weak rip current, are the dominant sediment transport mechanism in this sub-sample of the data set. Under low energy wave conditions, with no rip channel present, the onshore wave forcing was seen to be the governing mechanism of cross-shore sediment transport.

B. FOLLOW ON WORK

The BCDV directly and non-invasively measures, with a high temporal and spatial resolution, the hydrodynamic forces (turbulence and shear stress) which affect

suspended sediment transport. Employing a 1 cm resolution, the BDCV can accurately measure concentration and velocity profiles through 1 m of water to the wave induced boundary layer near the bed, providing robust measurements of the suspended sediment over various bottom types. The trade off associated with the 1 cm resolution is that the rolling grain bed-load, especially if in sheet flow, is only partially resolved. However, the rolling grain bed-load is forced by the same hydrodynamic effects as the sediment in suspension, presenting an opportunity for the use of models to improve estimates of bed-load transport.

Current empirical bed-load transport models are sensitive to the prediction of shear stress at the bed, τ_o (Natoo, Foster, Stanton, 2001). Direct measurement of velocity and shear stress profiles within the thin wave boundary layer provided by the BCDV can be applied to existing models, refining τ_o estimates and improving bed-load transport predictions. To this effect, follow on work should be conducted with the goal of translating the sediment flux profiles measured by the BCDV into model parameterizations.

LIST OF REFERENCES

Clay, C. S. and H. Medwin, Acoustical Oceanography: Principals and Applications, John Wiley & Sons, Ltd., New York, 1977.

Hewitt, P. G., Conceptual Physics (Ed. 5), Little, Brown, Boston, 1985.

Holman, R. Coastal Imaging Lab, Oregon State University, (http://cil-www.coas.oregonstate.edu/ncex/ncex.html).

Jonsson, I. G., Wave boundary layers and friction factors, *Proceedings of the 10th International Conference on Coastal Engineering, Tokyo*, 127-148, 1966.

Justesen, P., Turbulent wave boundary layers, *Series Paper 43, Institute of Hydrodynamic and Hydraulic Engineers, Technical University of Denmark*, 1988.

Kamphuis, J. W., Friction factors under oscillatory waves, *J Waterway Harbours Coastal Engineering Division, ASCE, vol. 101*, 135-144, 1975.

Liu, Z., Sediment Transport. Online book from www.weizmann.ac.il/ Literature-Online/Literature/Books/2001_Sediment_Transport.pdf., 37.

Natoo, P., Foster, D.L., and T. Stanton, Evaluation of three bed load transport models, *American Geophysical Union, EOS*, Fall Meeting, 2001.

Nielsen, P., Coastal Bottom Boundary Layers and Sediment Transport (Vol. 4). Singapore: World Scientific, 1992.

Sheilds, A., Anwendung der Aehnlickeitsmechanil und Turbulenzforchung auf die Geschiebebewegung, *Mitt Preuss Versuchsanstalt fur Wasserbau und Schiffbau*, no. 26, Berlin, 1936.

Stanton, T. P., Coherent Acoustic Sediment Flux Probe, US Army Corp of Engineers, Washington, DC, 1996.

Stanton, T. P., High resolution acoustic doppler profiling of velocity, Reynolds stresses and sediment concentration in wave forced boundary layers. Submitted to *Journal of Atmospheric and Oceanic Technology*, 2006.

Thorne, P. D., Constraining acoustic backscatter of suspended sediment concentration profiles using bed echo, *Journal of the Acoustical Society of America*, vol. 98, no. 4, 2280-2288, 1995.

Weltmer, M. A., Bed form evolution and sediment transport under breaking waves, *Master's Thesis, Naval Postgraduate School*, 2003.

INITIAL DISTRIBUTION LIST

1. Defense Technical Information Center
   Ft. Belvoir, Virginia

2. Dudley Knox Library
   Naval Postgraduate School
   Monterey, California

3. Dr. Donald P. Brutzman
   Naval Postgraduate School
   Monterey, California

4. Dr. Mary L. Batteen
   Naval Postgraduate School
   Monterey, California

5. VADM Roger Bacon, USN (Ret.)
   Naval Postgraduate School
   Monterey, California

6. CDR Denise Kruse, USN
   Naval Postgraduate School
   Monterey, California

7. Dr. Daphne Kapolka
   Naval Postgraduate School
   Monterey, California

8. Dr. Timothy Stanton
   Naval Postgraduate School
   Monterey, California

9. Dr. Edward Thornton
   Naval Postgraduate School
   Monterey, California

10. Mr. James Stockel
    Naval Postgraduate School
    Monterey, California